IEEE Access
Multidisciplinary | Rapid Review | Open Access Journal

Received January 21, 2018, accepted February 13, 2018, date of publication March 1, 2018, date of current version June 5, 2018.

Digital Object Identifier 10.1109/ACCESS.2018.2810204

Robust Optimal Control for Precision Improvement of Guided Gliding Vehicle Positioning

MOHSEN SAYADI, AMIRREZA KOSARI, (Member, IEEE), AND PARVIZ MOHAMMAD ZADEH
Faculty of New Sciences and Technologies, University of Tehran, Tehran 1417466191, Iran
Corresponding author: Amirreza Kosari (kosari_a@ut.ac.ir)

ABSTRACT In this paper, a new method for controlling and guidance of guided gliding vehicle (GGV) is provided. In this regard, a hybrid structure of nonlinear optimal control has been proposed to minimize control effort. The inner loop has a regulating function that guarantees the stability of motion and rotation equations and reduces the effect of external disturbances. The outer loop provides optimal tracking with a straight line scroll criterion for the GGV. The use of state dependent Riccati equation control involves determining the appropriate state dependent coefficient (SDC) form, which requires a complete understanding of the dynamics of the system. One of the methods for determining the relative dynamics of a nonlinear time-varying system and calculating SDC is the online identification method. The advantage of this method in determination of the SDC is more evident when it is not possible to fully understand the dynamics of the system or external factors and disturbance affect the system. This method also eliminates the problem of uncertainty and accurate measurement of parameters. In other words, it provides an adaptive model for different conditions. In this paper, the ANFIS network has been used for the first time for continuous and online identification of the system dynamics and calculating SDC. In order to ensure the stability of identification, the identifier will be trained first with the particle swarm optimization and the online back-propagation learning algorithm. The stability of the closed loop system with a proposed hybrid structure is investigated with the help of the Lyapunov function and the concept of passivity. The optimal and robust performance of the proposed framework has been investigated in terms of the ability to simultaneously pursue the target in the optimal path despite disturbance and optimize the control effort with multiple simulations.

INDEX TERMS ANFIS network, continuous online identification, guided glide vehicle (GGV), LOS guidance, nonlinear optimal control.

I. INTRODUCTION

During past decades, researchers' attention had been mainly focused on the development of UAVs with respect to control theories and their implementation. The unique characteristics of these aerial systems and their vast range of dimensions and capabilities have increased the demand of various industries and their comprehensive presence. In this respect, the guided glide vehicles (GGVs) have a significant potential to support missions and considerably reduce costs.

GGVs are a specific group of UAVs which are utilized for targets with low maneuverability since propulsion systems are removed. Under actuated states and lack of propulsion systems in dynamic systems, the inclusion of GGVs has caused many control problems, and the use of conventional methods faces some restrictions. The main factor for complexities in appropriate trajectory tracking control and stability analysis of these systems is their nonlinear input-output and non-minimum phase mapping [1]. Hence, GGV guidance, which is an especially challenging problem compared to other types of UAVs in this field, has attracted many researchers in recent years.

GGVs are employed for survivability, telecommunication, and military objectives. Hence, military applications have overshadowed control studies performed on these systems. Maximizing the level of range with guidance in the desired path [2] and real-time path planning based on the inverse dynamics [3] are the subjects of some of these studies. In these researches, the utilization of the real dynamic model system is necessary to achieve the appropriate results. The application of genetic algorithm for regulating PID controller

parameters is investigated by Attallah *et al*. [4]. However, the exerting of linear or linearized dynamic is the limitation of such methods. The modeling of linear free-fall flight in a windy environment is another attempt to simplify control problems and overcome upcoming challenges [5]. On the other hand, new differential glider equations based on optimal control are presented in order to maximize the final velocity at the objective point [6]. The assumption of a high-speed glider for overcoming gravitational effects is the major limitation of such researches.

The control of GGVs is generally defined as solving an optimization problem. In fact, the control scheme would overcome different obstacles during gliding by consuming the lowest energy and have to take the target with the minimum positioning error. By developing optimal nonlinear control theories and presenting practical methods for minimizing the cost function, Pearson presented the SDRE method in 1962 that was later developed by Wernti and Cook [7]. Simply, optimal linear control tactics are embedded in control schemes for nonlinear systems. For this purpose, system dynamics is first redefined into the state dependent coefficient (SDC) form by factorization. Finally, the online Riccati equation is solved for the optimal sub-problem solution related to the current moment's conditions. The SDC form gives more flexibility and action power to the designer compared to linearization around the nominal path [8]. On the other hand, the extraction of the appropriate SDC form that is able to satisfy controller design conditions always poses challenges [9]. Owing to the lack of practical solutions in choosing this form, SDC matrices are selected by designer intelligence with regard to the individual dynamics of each problem.

Along with the researchers in all engineering sciences, aerospace engineers have extensively used this method. The development of an advanced guidance law by Cloutier and Stansbery [10] and Cloutier and Zipfel [11] (1999), flight control and guidance of a pair of UAV leader-follower [12], [13], and the optimal guidance law for missile with control of state changes in impact with stationary surface targets [14] are some of these attempts. Designing an autopilot using the optimal control theory has evoked high interest till date [1], [15], [16]. In recent years, the incorporation of different control approaches with SDRE control to improve performance and implementation capability has been the objective of scholars. For instance, an integrator was augmented to SDRE to reduce the steady state error in the attitude control of super-maneuverable aircraft [17] and the SDRE control was incorporated with a sliding mode control for motion planning and end-effect control of multiple quad rotors under uncertainties and external disturbances [18]. The spacecraft and satellite controls are also amongst the interesting research fields [19]–[21].

Since the idea of identification with fuzzy structure in control systems was for the first time introduced by Takagi-Sugeno, many applications have been presented for utilizing ANFIS in identifying and improving control performances of complex nonlinear systems in the presence of uncertainties and unmodeled dynamics [22]. The results of simulations show the complete superiority of these controllers over conventional PIDs [23]. As a solution in aerial vehicles control, different methods are proposed based on neuro-fuzzy structures that are sometimes implemented in real conditions. Among them are the implementation of the heading control for UAV with delta wing [24] and the control of the passenger airplane model of NASA under uncertainties and compared to adaptive approaches [25]. The superiority of ANFIS nonlinear control does not require further parameter adjustments after training. Meanwhile, PID control, despite the simplicity of implementation in the real world, needs a high degree of experience in regulating the parameters and the best result is not obtained in all flight conditions [26]. The desired performance of positioning control of the UAV Aerosonde model with three fuzzy models is one of the other endeavors [27].

One of the most important ANFIS capabilities used in control algorithms is identification with this method. In online identification and nonlinear dynamic modeling, inverse dynamics would be identified for control purposes, since the delayed dynamic outputs are the inputs of ANFIS network [28]–[30]. In the case of propagating delayed control inputs, the identification of a direct model is conceivable. Identification can be considered for the whole system dynamics [31] and/or a part of it [32]. Besides, Al-Hadith *et al*. [31] modified the optimal control law corresponding to the identified discrete-time relation, and the high effectiveness of the ANFIS model is shown as well as the generality and simplicity of implementation. However, in both proposed configurations, the final approximation is a discrete-time one due to the nature of the input data and static and recursive essence of the identifier. On the other hand, various approaches are utilized in the online and offline training of ANFIS networks. Gradient-based methods [33], evolutionary algorithms such as GA [30], PSO [34] or their combination [35], [36], and training with neural networks included RBF [37] and, in some cases, the combination of classical and evolutionary methods [38] are some of the learning strategies.

The guidance systems can strongly reach various targets by distinct initial conditions. In these systems, a programmed algorithm is used that calculates angular positioning and the launch time for receiving the target. Designating the method of guidance and navigation depends on the aerial vehicle qualification and the communication type between flight systems [38]. Of the available guidance methods, line of sight (LOS) has the optimal performance especially for non-delayed communicating systems (or with a little time delay), stationary targets (or of low maneuverability), and in the absence of accelerometers [39]. This method endeavors to minimize the control attempt by determining the most optimized trajectory. In more detail, the guidance law in the LOS strategy involves the rewriting of the optimization problem for reducing tracking error. The aim of this method is to preserve the orientation of the aerial vehicle in the inter-

face line between the target and the aerial vehicle [38]–[40]. The mentioned line is the most optimized path possible in terms of time cost and control attempt. The benefits of this method are not only simplicity and effectiveness in practical implementation, but also no additional actuator and sensor are required.

A combination of two nested loops of SDRE is presented in this paper to overcome the physical and dynamical limitations of UAVs, especially GGVs. In the outer loop, the optimal guidance with LOS includes target tracking by means of minimizing the changed level in system orientation. However, the SDRE regulator in the inner loop tries to minimize the cost function with a minimum control attempt. The exclusive innovation of the proposed framework is driving the appropriate SDC form in each moment with online ANFIS identification. Online identification creates the probability of convergence of the approximation error of state matrices to zero in the presence of turbulence in the dynamic system. On the other hand, the initialization of the offline identifier with PSO is evidence of rapid convergence without trapping in local minimums. In this case, in addition to enhancing the robustness of the control scheme, the necessity of unexceptionable knowledge of system dynamics and turbulence, and the system's parameter identification are eliminated. The suggested control scheme ensures the stability and limiting of tracking errors related to the initial conditions in the case of a stable dynamic system of UAV without a propulsion system that is an essential constraint in dynamic design process.

The structure of this paper is as follows: First, the problem of nonlinear optimal control of SDRE is expressed in section 2. The UAV Dynamic Model is then introduced in section 3.

Generalities of the proposed control framework are presented in Section 4. Method of extracting SDC matrices by the ANFIS identifier are involved in section 5. In addition, the online update and offline dynamic detection method have been presented in this section. The control method for minimizing positioning error is discussed in section 6. The designing of the inner regulator and optimal guidance law are involved in this section. In Section 7, stability analysis and its conditions are described in detail. In Section 8, multiple simulations are done to verify the effects of the recommended control framework and the level of its robustness under external turbulence. Finally, the concluding remarks of this study are contained in Section 9.

II. SDRE NONLINEAR CONTROL

A. SDC PARAMETERIZATION

The SDC structure is a factorization method that shows a nonlinear system in a linear-like form. Consider the nonlinear system (1).

$$\dot{\boldsymbol{x}}(t) = \boldsymbol{f}(\boldsymbol{x}) + \boldsymbol{B}(\boldsymbol{x})\boldsymbol{u}(t) + \boldsymbol{F}(\boldsymbol{x}, t), \boldsymbol{x}(\boldsymbol{0}) = \boldsymbol{x_0} \quad (1)$$

where, $\boldsymbol{x} \in \boldsymbol{R^n}$, $\boldsymbol{u} \in \boldsymbol{R^m}$ are the vector of state and input control variables, **respectively**, $\boldsymbol{x_0}$ is the vector of initial state variables, $\boldsymbol{f}(\boldsymbol{x}) : \boldsymbol{R^n} \rightarrow \boldsymbol{R^n}$, $\boldsymbol{B}(\boldsymbol{x}) : \boldsymbol{R^n} \rightarrow \boldsymbol{R^{n\times m}}$ where, $(\forall \boldsymbol{x}, \boldsymbol{B}(\boldsymbol{x}) \neq 0)$ and $\boldsymbol{F}(\boldsymbol{x}, \boldsymbol{t})$ is the vector of other nonlinear terms.

If $\boldsymbol{f}(\boldsymbol{x})$ is differentiable, then the nonlinear continuous matrix $\boldsymbol{A}(\boldsymbol{x})$ is obtained from (2).

$$\boldsymbol{A}(\boldsymbol{x}) = \boldsymbol{f}(\boldsymbol{x})/\boldsymbol{x}(\boldsymbol{t}) \quad (2)$$

$A(x)$ is an $n \times n$ matrix derived from mathematical factorization methods and is not unique for $n > 1$. With these definitions, the linear-like system obtained from the nonlinear system (1) is obtained as (3).

$$\dot{\boldsymbol{x}}(\boldsymbol{t}) = \boldsymbol{A}(\boldsymbol{x})\boldsymbol{x}(\boldsymbol{t}) + \boldsymbol{B}(\boldsymbol{x})\boldsymbol{u}(\boldsymbol{t}) + \boldsymbol{F}(\boldsymbol{x}.\boldsymbol{t})\, \boldsymbol{t} > \boldsymbol{0}; \quad \boldsymbol{x}(\boldsymbol{0}) = \boldsymbol{x_0} \quad (3)$$

where, $A(x)$ and $B(x)$ are SDC matrices that at any time of t_c, the system dynamics can be considered in a linear-like form with fixed matrices $A(x(t_c))$ and $B(x(t_c))$, thus suitable linear control theories can be applied.

B. CONTROL PROBLEM FORMULATION

For the optimal control problem of the nonlinear system (3), the control input is designed to minimize the cost function (4):

$$\boldsymbol{J}(\boldsymbol{x_0}, \boldsymbol{u}) = \frac{\boldsymbol{1}}{\boldsymbol{2}} \int_{\boldsymbol{0}}^{\infty} \left\{ \boldsymbol{x^T}(\boldsymbol{t})\boldsymbol{Q_x}(\boldsymbol{x})\boldsymbol{x}(\boldsymbol{t}) + \boldsymbol{u^T}(\boldsymbol{t})\boldsymbol{R_x}(\boldsymbol{x})\boldsymbol{u}(\boldsymbol{t}) \right\} \boldsymbol{dt} \quad (4)$$

where, the matrices $Q_x(x) : R^n \rightarrow R^{n\times n}$ and $R_x(x) : R^n \rightarrow R^{n\times m}$ are symmetric positive semi-definite and positive definite matrices, respectively. Weight state-dependent matrices $Q_x(x)$ and $R_x(x)$ are design parameters for the estimation of state variables and control signals. In fact, the choice of weight matrices has become an effective factor on the quality of the system response. Physically, larger $R_x(x)$ matrix affects the stability of the system associated with reduced response speed and increased tracking error. Selecting large values for this matrix will be accompanied by operator saturation. On the other hand, the large values of the matrix $Q_x(x)$ are stabilize the system at the minimum cost of the state variables or in other words, a reduction in the convergence time and error rate. However, the large values of this matrix increase control effort.

For the nonlinear system described in (3), the control rule for the infinite problem will exist in form (5) [7].

$$\boldsymbol{u}(\boldsymbol{x}) = -\boldsymbol{K_x}(\boldsymbol{x})\boldsymbol{x}(\boldsymbol{t}) \quad (5)$$

where, $K_x(x) = R_x^{-1}(x)B^T(x)P_x(x)$ and $\forall x \in R^n$, the matrix $P_x(x)$ is the positive definite unique solution for the Riccati equation (6).

$$\boldsymbol{P_x}(\boldsymbol{x})\boldsymbol{A}(\boldsymbol{x}) + \boldsymbol{A^T}(\boldsymbol{x})\boldsymbol{P_x}(\boldsymbol{x}) - \boldsymbol{P_x}(\boldsymbol{x})\boldsymbol{B}(\boldsymbol{x})\boldsymbol{R_x^{-1}}(\boldsymbol{x})\boldsymbol{B^T}(\boldsymbol{x}) \times \boldsymbol{P_x}(\boldsymbol{x}) + \boldsymbol{Q_x}(\boldsymbol{x}) = \boldsymbol{0} \quad (6)$$

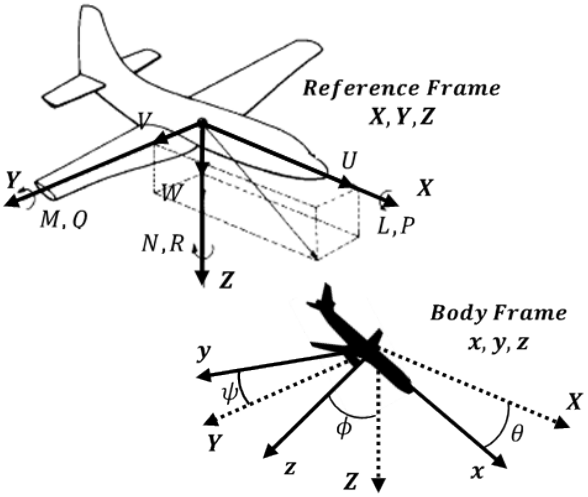

FIGURE 1. System coordinate and dynamic variable definition.

III. DYNAMIC SYSTEM MODELING

The promising controller design relies on exploiting an appropriate dynamic model for problem formulation. These dynamics can be attributed to the system's real behavior and could simulate simplicity. Utilizing Newton's second law can lead to a simpler closed form than other dynamic modeling approaches. Considering Newton's second law, the employment of linear and angular momentum easily shows that GGV's 6 DOF nonlinear dynamic equations of motion at the release point coordination (Fig. 1) can be expressed as (7) [4].

$$\begin{aligned}
\dot{U} &= -QW + VR - g\sin(\theta) + \frac{F_{Ax}}{m} \\
\dot{V} &= -RU + PW + g\cos(\theta)\sin(\phi) + \frac{F_{Ay}}{m} \\
\dot{W} &= -PV + QU + g\cos(\theta)\cos(\phi) + \frac{F_{Az}}{m} \\
\dot{Q} &= \frac{1}{I_{yy}}\left[(I_{zz} - I_{xx})PR + I_{xz}\left(R^2 - P^2\right) + M_A\right] \\
\begin{Bmatrix} \dot{P} \\ \dot{R} \end{Bmatrix} &= \frac{1}{I_{xx}I_{zz} - I_{xz}^2}\begin{bmatrix} I_{zz} & I_{xz} \\ I_{xz} & I_{xx} \end{bmatrix} \\
&\quad \times \begin{Bmatrix} I_{xz}PQ + (I_{yy} - I_{zz})RQ + L_A \\ -I_{xz}QR + (I_{xx} - I_{yy})PQ + N_A \end{Bmatrix}
\end{aligned} \tag{7}$$

where, $\{U, V, W\}$ are linear velocities and $\{P, Q, R\}$ are angular velocities in line with axes x, y and z. M and g are the UAV's mass and gravity acceleration and θ, ϕ, and ψ are the Euler angles. Subscript A and subscript i refer to aerodynamic and the direction of motion. F represents forces while L, M, and N denote the torques applied to aircraft, too. Substituting forces and torques in relation to y(7) and some simplification, 6DOF dynamic equations of GGV are obtained [41].

The dynamics governing the angles and positions of the GGV considering its dynamics are expressed in the form of equations (8) and (9).

$$\begin{bmatrix} \dot{\theta} \\ \dot{\phi} \\ \dot{\psi} \end{bmatrix} = \begin{bmatrix} 0 & \cos\phi & -\sin\phi \\ 1 & \cos\phi\tan\theta & \sin\phi\tan\theta \\ 0 & \cos\phi\sec\theta & \sin\phi\sec\theta \end{bmatrix} \begin{bmatrix} P \\ Q \\ R \end{bmatrix} \tag{8}$$

$$\begin{bmatrix} \dot{x} \\ \dot{y} \\ \dot{z} \end{bmatrix} = \begin{bmatrix} \cos\psi & -\sin\psi & 0 \\ \sin\psi & \cos\psi & 0 \\ 0 & 0 & 1 \end{bmatrix} \begin{bmatrix} \cos\theta & 0 & \sin\theta \\ 0 & 1 & 0 \\ -\sin\theta & 0 & \cos\theta \end{bmatrix} \times \begin{bmatrix} 1 & 0 & 0 \\ 0 & \cos\phi & -\sin\phi \\ 0 & \sin\phi & \cos\phi \end{bmatrix} \begin{bmatrix} U \\ V \\ W \end{bmatrix} \tag{9}$$

Given the forces and aerodynamic moments, Equations (7) can be represented in the general form (10).

$$\dot{x}_{in} = f(x_{in}) + B(x_{in})u_{in}(t) \tag{10}$$

where, $x_{in} = \begin{bmatrix} U & V & W & P & Q & R \end{bmatrix}^T \in R^{n_{in}}$ are the system states, $u_{in} = \begin{bmatrix} \delta_a & \delta_e & \delta_r & \delta_T \end{bmatrix}^T \in R^{m_{in}}$ are vehicle control surfaces, $f(x_{in}) : R^{n_{in}} \rightarrow R^{n_{in}}$ and $B(x_{in}) : R^{n_{in}} \rightarrow R^{n_{in} \times m_{in}}$.

IV. METHODOLOGY

The SDRE Double-Loop Control Framework, with the online SDC calculation at any given moment resulted in optimal control and closed loop system resistance. Consequently, GGV is positioned more precisely in spite of adverse weather conditions, and target tracking is done with less error. Figure 2 shows the general view of this structure.

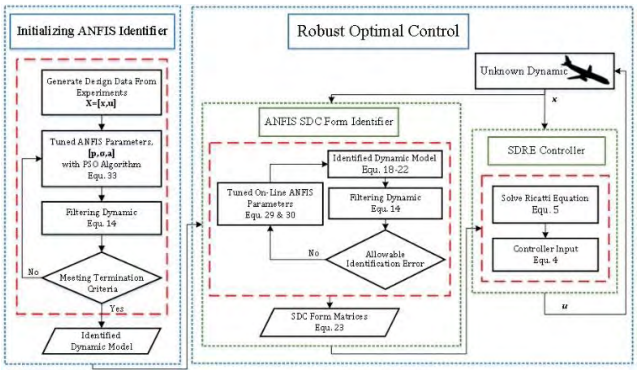

FIGURE 2. Robust optimal control framework.

According to this figure, the proposed framework can be upgraded to control performances in two stages. In the first stage, the GGV dynamic would be initialized and identified by an offline ANFIS network based on an acquired database tuned by the PSO algorithm. The second stage of the GGV control concentrates on target tracking. In this stage, while the state matrices of the SDC form are determined, based on the initial identified model, the SDRE controller reshapes the robust optimal control input to hold the GGV in the desired path. In fact, the optimal control phase is a nested architecture that ensures guidance of the GGV toward the target and, furthermore, optimizes control efforts and state regulation. If the allowable identification tolerance is not satisfied, the ANFIS identifier parameters have to be adopted online. The details

of the suggested control framework and its advantages are described in the next section.

V. DYNAMIC REDEFINITION, SDC FORMULATION

The use of a nonlinear regulator (5) depends on the representation of the dynamic equations of nonlinear systems in a form similar to (3).

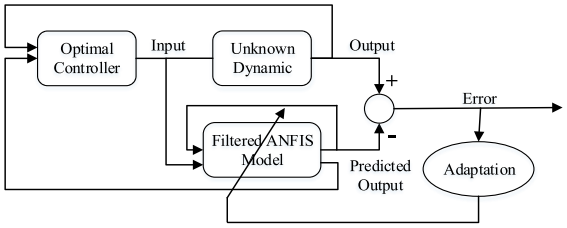

FIGURE 3. Structure of unknown dynamic online identification.

The determination of the appropriate form of SDC for dynamic (10) demands complete identification of the system, adequate knowledge of the dynamic parameters, and, maybe, the modeling of existing uncertainties not conceivable in reality. Hence, online identification, which finds an approximated model of time-variant nonlinear dynamic, is a promising solution. It means that the GGV dynamic is identified to improve the performance and robustness of the controller at each moment (Fig. 3). The main circumscription of the identification methods in this issue is the extraction of a high-precision linear corresponding model (3) for replacement with the complex nonlinear dynamic of GGV. This factor severely limits selection identification techniques. However, the concurrent use of neural and fuzzy network capabilities in the ANFIS network amplifies the identification power of this structure. On the other hand, the matrices of A and B can be determined according to GGV's condition at any moment. As a result of the linear outer layer of this model. It should be noted that A and B are not exactly equal to the matrices in the main dynamic but will be selected so that the identifier output is coincidental with the output of the real dynamic.

A set of input and output data is necessary for training the ANFIS network. According to (10), network inputs are state and control inputs of real dynamic ($X = [x_{in}.u_{in}]$) and its outputs are the derivative of state variables $\dot{\boldsymbol{x}}$. The current issue's outputs are linear and angular accelerations. Use of the observer in the absence of an accelerometer and/or filtering method is essential. Filtering is a prevalent method, when static neural networks are approximated dynamic functions. In these methods, the static and dynamic parts are separated from each other and the integration of their output can present a dynamic relation. In such a structure, the network merely identifies the static part. Thus, the needs for the derivatives of output variables or design observation are obviated. The fuzzy-neural nature of ANFIS networks, inspiration from dynamic filtering, and online continuous training of the ANFIS network as the identifier are presented for the first time in this paper.

A. FILTERING DYNAMIC

A nonlinear system (10) can be considered as the following:

$$\dot{\boldsymbol{x}} = g(x.u) \tag{11}$$

where u is inputs vector and x is state vector of the system and g is also an unknown function that must be identified. Adding $\pm Hx$ to and subtracting from (11) where H is an arbitrary Hurwitz matrix:

$$\dot{\boldsymbol{x}} = Hx + h(x.u) \tag{12}$$

that

$$h\,(x.u) = g\,(x.u) - Hx \tag{13}$$

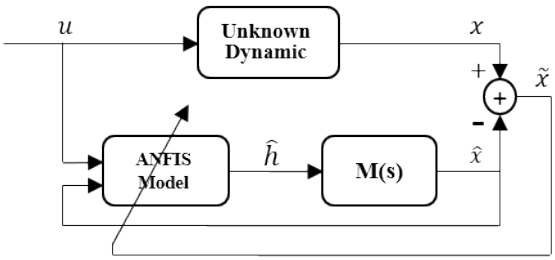

FIGURE 4. Using filtering in ANFIS identifier.

Figure 4 shows the method of identification and the use of the dynamic term for static identification. Stable transfer function $M\,(s) = (sI - H)^{-1}$ is equivalent to the dynamic part and integral operator. For detailed information about filtering, please refer to Talebi *et al*. [42] (2009).

Finally, the identified equation of the system dynamic (10) is:

$$\dot{\hat{\boldsymbol{x}}} = \hat{\boldsymbol{h}}\left(\hat{\boldsymbol{x}}.u\right) + H\hat{\boldsymbol{x}} \tag{14}$$

This method rectifies the need for recursive network and storage of delayed data, so the identified dynamic is continuous.

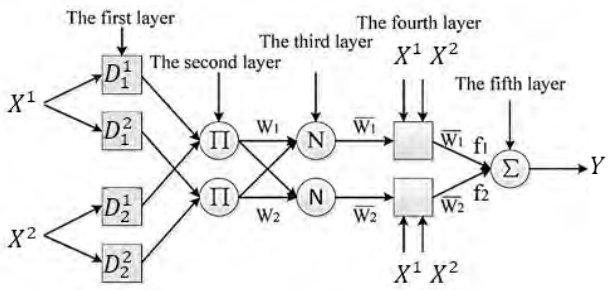

FIGURE 5. ANFIS multi-layer block diagram.

B. ONLINE ADAPTATION OF STATIC ANFIS

The ANFIS model partitions the input space into small local regions for approximation of complex nonlinear systems, yielding simpler approximated models for each region. The ANFIS structure is shown in Fig. 5 for function approximation with two inputs and the assumption of two

fuzzy rules. For example, the output for the two inputs X^1 and X^2 is:

$$\begin{aligned} &Rule1: \ if\ X^1\ is\ A_1^1\ and\ X^2 A_1^2.\ then\ f_1 = p_1^1 X^1 + p_1^2 X^2 + p_1^3 \\ &Rule2: \ if\ X^1\ is\ A_2^1\ and\ X^2 A_2^2.\ then\ f_2 = p_2^1 X^1 + p_2^2 X^2 + p_2^3 \end{aligned} \tag{15}$$

As seen in Fig. 5, the structure has two separate parts: first, the antecedent part and then the inference part. These two parts are related by fuzzy rules in the network bed. The final network has adaptive topology equivalent to Sugeno Fuzzy Inference System. In this five-layer network, only the first and fourth layers are trained. The only limitation to using this structure is its one-dimensional output. So, for any state an individual ANFIS network has to be designed.

The parameters of the first fuzzy layer are called premise parameters. In any appropriate fuzzy membership function including Gaussian membership function, c_i^j and σ_i^j are the values of center and standard deviations for each input X^j from the i-th Gaussian membership function. The output of the i-th node in this layer is in the following form:

$$\begin{aligned} O_{1i}^j &= \mu D_i^j(X) \\ \mu D_i^j(X) &= exp\left(-\frac{1}{2}\left(\frac{X^j - c_i^j}{\sigma_i^j}\right)^{-2}\right) \end{aligned} \tag{16}$$

The output of second layer that is called the firing strength is the multiplication of the previous layer output.

$$O_{2i} = w_i = \prod_j \mu D_i^j(X) \tag{17}$$

Normalized firing strength is the output of next layer that normalizes the previous layer output.

$$O_{3i} = \bar{w}_i = \frac{w_i}{\sum_i^r w_i} \tag{18}$$

where r is the number of fuzzy rules equivalent to the number of membership functions. The output of the fourth adaptive layer, the defuzzy layer, is described in the following relation:

$$O_{4i} = \bar{w}_i f_i = \bar{w}_i \sum_j p_i^j \chi^j \tag{19}$$

where $\chi = [X1]$ unit value is added as a bias effect. In these linear nodes, p_i^j coefficients, known as consequent parameters, should also be adapted. The overall output in the fifth layer is a summation of all incoming signals from the previous layer.

$$O_{5i} = \sum_i \bar{w}_i f_i \tag{20}$$

The identification with this structure, the identified matrices $\hat{\boldsymbol{A}}$ and $\hat{\boldsymbol{B}}$, and the vector $\hat{\boldsymbol{F}}$ are equal to:

$$\begin{aligned} \hat{\boldsymbol{A}} &= \bar{w}^T p^{j=1.n} + H \\ \hat{\boldsymbol{B}} &= \bar{w}^T p^{j=n+1.n+m} \\ \hat{\boldsymbol{F}} &= \bar{w}^T p^{n+m+1} \end{aligned} \tag{21}$$

Adapting ANFIS network parameters is an optimization problem. Hence, both the groups of optimization methods such as gradient base and population base and/or their combined methods are used for this purpose. While, a high response speed and online training is required for this problem, using heuristic methods and complex hybrid methods of gradient base is not intelligent decision. The gradient decent method has lower complexity and computational cost than other training ANFIS structure algorithm [43].

For consequent parameters in the i-th node, the updated formula based on modified back-propagation algorithm is defined as

$$\dot{\hat{\boldsymbol{p}}}_i = -\eta_i \frac{\partial J}{\partial \hat{\boldsymbol{p}}_i} - \rho_i \|\tilde{y}\| \hat{\boldsymbol{p}}_i \tag{22}$$

where $\tilde{y}$, J, and η_i are identification error, error function and positive learning constant, respectively. The second term, called the momentum term, is improved for design robustness. This term increases error convergence acceleration in a back-propagation strategy without changing constant learning. In general, if learning data do not have sufficient precision for some reason, the weights of network oscillate and do not converge on its optimal and appropriate value. This method highly obviates this defect by adjusting parameters based on parameter values in the previous iteration and error value. However, ρ is a small and positive constant. In this regard, the modified back-propagation algorithm has better proficiency in identifying complex nonlinear functions [44].

The error function can be expressed as:

$$J = \frac{1}{2}\tilde{y}^T \tilde{y} \tag{23}$$

The employment of the chain rule, considering the ANFIS structure and some simplification computations (24), can be derived as

$$\frac{\partial J}{\partial \hat{\boldsymbol{p}}_i} = -\tilde{y}^T \frac{\partial \hat{\boldsymbol{y}}}{\partial Y} \frac{\partial Y}{\partial \hat{\boldsymbol{p}}_i} \tag{24}$$

$(\partial y^\wedge)/\partial Y$ is calculated on the assumption that identification is based on identified output (Fig. 4), which is called static back propagation, and so it is assumed that $\dot{\hat{\boldsymbol{y}}} = 0$. Therefore:

$$\frac{\partial \hat{\boldsymbol{y}}}{\partial Y} = -H^{-1} \tag{25}$$

The relationship (24) can be replaced with a simplified form (26) by the characteristics of the structure of multi-layer network ANFIS

$$\frac{\partial J}{\partial \hat{\boldsymbol{p}}_i} = \tilde{y}^T H^{-1} \bar{W}_i [X1] \tag{26}$$

Bias terms would be concluded by adding a unit vector. Consequently, the adaptation law for consequent parameters is equivalent to:

$$\dot{\hat{\boldsymbol{p}}}_i = -\eta_i \tilde{y}^T H^{-1} \bar{W}_i [X1] - \rho_i \|\tilde{y}\| \hat{\boldsymbol{p}}_i \tag{27}$$

The selection of the appropriate value of learning rate is of high importance because of its direct influence on convergence and stability. High learning rate will reduce the stability

of the system by improving convergence. On the other hand, smaller values for the learning rate disturbed convergence against improved stability assurance [45] This methodology can be also used for updating premise parameters matrices c and σ, thus:

$$\dot{\hat{\boldsymbol{c}}} = \eta_c \tilde{y}^T \frac{\partial \hat{\boldsymbol{y}}}{\partial Y} \frac{\partial Y}{\partial \bar{w}} \frac{\partial \bar{w}}{\partial w} \frac{\partial w}{\partial \hat{\boldsymbol{c}}} - \rho_c \|\tilde{y}\| \hat{\boldsymbol{c}}$$
$$\dot{\hat{\boldsymbol{\sigma}}} 85 = \eta_\sigma \tilde{y}^T \frac{\partial \hat{\boldsymbol{y}}}{\partial Y} \frac{\partial Y}{\partial \bar{w}} \frac{\partial \bar{w}}{\partial w} \frac{\partial w}{\partial \hat{\boldsymbol{\sigma}}} - \rho_\sigma \|\tilde{y}\| \hat{\boldsymbol{\sigma}} \quad (28)$$

Considering (18) and (19), it can be easily shown that:

$$\frac{\partial Y}{\partial \bar{w}} = \Lambda\left([f_1. \ \ldots \ .f_i. \ \ldots \ .f_m]^T\right)$$
$$\begin{cases} \frac{\partial \bar{w}_j}{\partial w_k} = \frac{\sum_{l=1}^{r} w_l - w_i}{\left(\sum_{l=1}^{r} w_l\right)^2} j = k \\ \frac{\partial \bar{w}_j}{\partial w_k} = \frac{-w_j}{\left(\sum_{l=1}^{r} w_l\right)^2} j \neq k \end{cases} \quad (29)$$

where the subscript "m" represents the number of fuzzy rules and $\Lambda(\cdot)$ is the diagonalization operator of the vector $[f_1. \ \ldots \ .f_i. \ \ldots \ .f_m]^T$. With layer definition (16) and (17) and after simplification, adaptation laws take the form

$$\frac{\partial w}{\partial \hat{\boldsymbol{c}}_{ij}} = \frac{x_j - \hat{\boldsymbol{c}}_{ij}}{\left(\sigma_{ij}\right)^2} w_i$$
$$\frac{\partial w}{\partial a_{ij}} = \frac{\left(x_j - \hat{\boldsymbol{c}}_{ij}\right)^2}{\sigma_{ij}^3} w_i \quad (30)$$

Substituting (29) and (30) to (28) results in a simplified form.

Although the back-propagation method has high power, this performance is dependent on the initial values and there is the possibility of trapping into local minimums. Unfortunately, online updating is associated with high computational costs and can cause high errors and oscillations in the primary moments. In presence of the fuzzy inference system, it can be expected that the necessity of updating network during control process is considerably reduced with appropriate initial training of the ANFIS network. In this case, all the mentioned defects including the probability of trapping in local minimums and high computational costs are resolved in the primary moments.

Hence, a set of stored input and output data in various conditions can be initially trained for the ANFIS network. The training set should contain rich data that describe the full behavior of the system and decrease identification error. In this stage, evolutionary algorithms can be used to achieve a high degree of precision and avoid local minimums since there is no time limit. The particle swarm optimization (PSO) is one of the optimization algorithms whose individual characteristics have attracted much attention in recent years [30], [46], [47]. Finding high quality solutions within short computational time compared to other optimization heuristic algorithms [48] ensuring stable convergence, and approximating more appropriate input-output relation in highly complex problems [33], [49] are some of reasons for developing this method.

C. PSO TUNED INITIAL ANFIS

The PSO method is a parallel evolutionary computational algorithm that was developed by Kennedy and Eberhart [50] in 1995, based on choreography of birds and fishes in finding food sources. Initially, populations are initialized based on randomized selection. Each particle of population is allocated a position and velocity that make its movement possible toward an optimal solution. The position of each particle in the design space is referred to the bounds of design variables. In each iteration, particle velocity and position is updated considering the personal best P_{best}, global best g_{best} and the velocity in the previous iteration. Mathematically, velocity, v and position, x in $k+1$th iteration are:

$$v_{k+1} = wv_k + c_1 r_1 (P_{best} - x_k) + c_2 r_2 (g_{best} - x_k)$$
$$x_{k+1} = x_k + v_{k+1} \quad (31)$$

where w is inertia weight, c_1 and c_2 are positive acceleration constants, and the parameters r_1 and r_2 are random values between 0 and 1. The global best has the optimum value of cost function compared to other positions. The searching iteration is repeated until any termination conditions are met and convergence is obtained.

The mutation operator is employed like a genetic algorithm, decreasing the probability of trapping in local minimums. This operator deduces its range of action over time. In addition, particle velocity is restricted to search space boundaries. In case any particle passes through the design space, the related position element is modified to maintain position inside the design space.

The set of premise and consequent parameters $[c\sigma p]$ are design variables in training the ANFIS structure.

For the reasons mentioned earlier, dynamic filtering is also necessary here. In this offline training, the error function is considered as the mean square error (MSE). The optimization process is terminated when the value of error function achieves an acceptable level.

The stability of the PSO method as the optimizer in training ANFIS identifier is assured with some constraints on the inertia coefficient, acceleration constants, and learning constant [51]. Such conditions are considered in addressing this problem.

VI. ROBUST OPTIMAL CONTROL FRAMEWORK

The primary purposes of the controller design for UAVs are the reduction of target tracking error and time consumption along with the ensuring of stability and robustness. This problem is faced with additional challenges in the case of GGVs because of omitting propulsion systems. The small dimensions of this category make stability a problem particularly in the presence of disturbances and magnify tracking error. The other point is the quiddity of the under-actuated and non-minimum phases of these systems that limit the use of control methods.

The control objectives can be met with the State-Dependent Riccati Equation (SDRE) method. This method

has interested engineers more than other optimal control techniques since the propounding of an effective algorithm for nonlinear feedback control and high design flexibility by selecting weighted matrices. It can be argued that the foremost advantage of this controller is the possibility of compromising between control effort, admissible state errors, and fast error convergence owing to the adjustment of weighting matrices [10].

In this section, the control framework is designed and its performance is perused in terms of stability and the level of tracking error. The SDRE controller is designed in two inner and outer loops by guidance with the LOS method for convergence of the target tracking error to the lowest level in an acceptable distance. The inner loop regulates the states in the zero criterion, and the outer loop reclaims the optimal path to explore the target LOS. The results of both loops are to preserve the system in the optimal path and confront with each kind of diversion from the optimum condition.

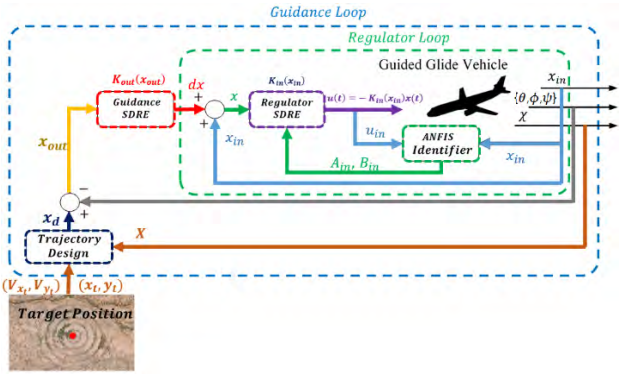

FIGURE 6. The overall block diagram of the proposed approach.

Figure 6 shows a general diagram of the proposed control method. In this diagram, the ANFIS network, in accordance with the previous section, calculates the SDC matrices for dynamics (10) at any point by receiving linear and angular velocity values from the sensor, and provides the controller for the inner loop. The inner loop has a regulating function, which ensures the stability of motion and rotation equations and reduces the effect of external disturbances. In this loop, the linear and angular velocity information of the system are measured and the internal loop gain are calculated. At the same time, the outer loop generates the desired angular velocity as a guidance signal by receiving tracking error information, which is applied as a mandatory input to the inner loop controller. Then, in the inner loop, the final control signal is determined according to the mandatory input and the gain of the inner loop controller. Eventually, after the GVV is placed on the target's path, the output of the outer loop controller will be zero and the inner loop controller continues its path by stabilizing the angular velocities. As long as the tracking error is zero, no change in the angular velocity is generated and the GVV continues to move at the desired angle to reach the target.

The design of the inner loop controller and the optimal guidance in the outer loop according to this structure are described in details therein.

A. SDRE INNER LOOP

The main purpose of the controller design for GGVs is minimizing control effort in spite of sustaining target tracking error at an acceptable level. This purpose is the genuine aim of optimal control (5). Nonlinear regulator (5) ascertains this by maintaining state constantly at any moment. The controller absolutely rejects any turbulence in angular velocities. Therefore, GGV could keep its orientation in the desired path after transition time for any initial condition.

Therefore, in accordance with Fig. 6 after online computation of the SDC matrices, the inner loop control rule is presented as (32).

$$u(x) = -K_{in}(x_{in})\, x(t) \tag{32}$$

where, $K_{in}(x_{in}) = R_{in}^{-1}(x_{in})\, B_{in}^{T}(x_{in})\, P_{in}(x_{in})$ is the gain of the controller of the inner loop; $x \in R^{n_{in}}$ is the sum signal of the values of linear and angular velocities by sensors; deviations are $(x = x_{in} + dx)$. The deviations dx include all mandatory external disturbances which are imposed by the outer loop guidance rule for guiding GGV.

Here, $P_{in}(x_{in})$ is a positive definitive and symmetric matrix obtained from solving the Riccati equation (33) where the matrices $A_{in}(x_{in})$ and $B_{in}(x_{in})$ are the same SDC matrices obtained at any time from the ANFIS network.

$$P_{in}(x_{in})\, A_{in}(x_{in}) + A_{in}^{T}(x_{in})\, P_{in}(x_{in}) - P_{in}(x_{in})\, B_{in}(x_{in}) \times R_{in}^{-1}(x_{in})\, B_{in}^{T}(x_{in})\, P_{in}(x_{in}) + Q_{in}(x_{in}) = 0 \tag{33}$$

$Q_{in}(x_{in}) : R^{n_{in}} \to R^{n_{in} \times n_{in}}$ and $R_{in}(x_{in}) : R^{n_{in}} \to R^{n_{in} \times m_{in}}$ are weight matrices related to the objective function of the inner loop.

B. OPTIMAL GUIDANCE LAW

LOS guidance is one of the applicable methods that satisfy design criteria including production cost, implementation capability, efficiency, and tolerable maneuverability for GGV. This method maintains the relative velocity vector of GGV in each moment tangent to the line passing the target. In other words, target LOS is the optimum flight trajectory of GGV. This issue necessitates that the rate of LOS rotation tends to zero using the aileron and rudder commands.

The guidance law in this approach is designed online, based on the error of the vehicle's angular position with LOS (Fig. 7). Accordingly, the optimum orientation signals values in time t are mathematically equal to:

$$\theta_d(t) = -tan^{-1}\left(\frac{Z_a(t)}{X_t(t) - X_a(t)}\right) + \alpha(t) \tag{34}$$

where θ_d is the desired pitch angle, Z_a is the altitude, X_t and X_a are the positions of the target and GGV in the X direction, respectively. α is the angle of attack related to LOS.

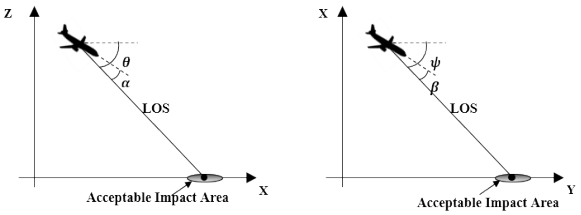

FIGURE 7. Guidance strategy for tracking target.

So, the desired Yaw angle ψ_d is defined as:

$$\psi_d(t) = tan^{-1}\left(\frac{Y_t\,(t) - Y_a\,(t)}{X_t\,(t) - X_a\,(t)}\right) + \beta(t) \tag{35}$$

where Y_t and Y_a are target and GGV positions in the direction of Y and β is the side slip.

For the GGV to continue to move in a desirable direction it is necessary for the GGV angles to reach the desired angles in the line of sight. In this case, the GGV continues its path until it hits the target by maintaining angular velocities of the inner loop controller. The tracking problem in the outer loop can be considered as tracking error stabilization problem. The model of the tracking error is shown in (36).

$$\dot{x}_{out}\,(t) = \begin{bmatrix} 0 & cose_\varphi & -sine_\varphi \\ 1 & cose_\varphi tane_\theta & sine_\varphi tane_\theta \\ 0 & cose_\varphi sece_\theta & sine_\varphi sece_\theta \end{bmatrix} u_{out}(t) \tag{36}$$

In this relationship, $x_{out} \in R^{n_{out}}$ is the tracking error vector and $u_{out} \in R^{m_{out}}$ is the control signal of the outer loop, defined as (37) and (38).

$$x_{out} = \begin{bmatrix} e_\theta \\ e_\varphi \\ e_\psi \end{bmatrix} = \begin{bmatrix} \theta_d - \theta \\ \varphi_d - \varphi \\ \psi_d - \psi \end{bmatrix} \tag{37}$$

$$u_{out} = dx = \begin{bmatrix} p_d \\ q_d \\ r_d \end{bmatrix} \tag{38}$$

The dynamic tracking error is in the SDC form, thus the outer loop control rule is obtained as (39).

$$u_{out}\,(t) = -K_{out}(x_{out})x_{out}(t) \tag{39}$$

where

$$K_{out}\,(x_{out}) = R_{out}^{-1}(x_{out})B_{out}^{T}(x_{out})P_{out}(x_{out})$$

Given the SDC form, the outer loop of the linear-like matrix is $A_{out} = 0$. Therefore, the system's controllability is easily verifiable, and the Riccati equation for this section is simplified as (40).

$$-P_{out}\,(x_{out})\,B_{out}\,(x_{out})\,R_{out}^{-1}\,(x_{out})\,B_{out}^{T}\,(x_{out})\,P_{out}\,(x_{out}) + Q_{out}\,(x_{out}) = 0 \tag{40}$$

where;

$$B_{out} = \begin{bmatrix} 0 & cos(e_\phi) & -sin(e_\phi) \\ 1 & sin(e_\phi)tan(e_\theta) & cos(e_\phi)tan(e_\theta) \\ 0 & sin(e_\phi)sec(e_\theta) & cos(e_\phi)sec(e_\theta) \end{bmatrix}$$

and $Q_{out}\,(x_{out}) : R^{n_{out}} \rightarrow R^{n_{out}\times n_{out}}$ and $R_{out}\,(x_{out}) : R^{n_{out}} \rightarrow R^{n_{out}\times m_{out}}$ are the weight matrices related to the objective function of the outer loop.

In accordance with Fig. 6, angular velocities must be determined in such a way that the difference between the angular position of the GGV and the reference path is zero. This goal is consistent with the overall performance of the SDRE regulator. In this case, by adding the angular velocity determined in this loop as an external disturbance of the outer loop, the inner loop regulator moves the control variables (displacement of control surfaces) in a direction so that the GGV maintains its direction in the reference path.

VII. CONTROLLABILITY AND DYNAMIC STABILITY ANALYSIS

A. CONTROLLABILITY ANALYSIS

For infinite-horizon optimal control problems, the linear system must be completely controllable. Controllability ensures the settlement of the optimal cost. Otherwise, the cost function value diverges (infinite) and it is meaningless to consider optimal performance for controller. The linear system is controllable, if all the columns of the controllability matrix are linearly independent (41).

$$\left[B\;AB\;\ldots\;A^{n-1}\;B\right] \tag{41}$$

This is equivalent to being Hurwitz for a closed-loop matrix $A_{cl} = A - BK$. With regard to the used approach and the assumption of system linearity in each moment, which means changing the value of A(x) and B(x), controllability must be guaranteed for $\forall x$ in the design space. Assuming the controllability of the pair of matrices A (x (t_c)) and B (x (t_c)) in each moment t_c, the control law (5) exists [52].

Cloutier *et al*. [53] proved that if $\forall x$ is a symmetric A_{cl} (x) matrix, the global stability of this method is assured. There are some heavy constraints for SDRE control stability that being locally Lipchitz for the A, B and C matrices is one of controllability condition. This means roundedness of these matrix functions poses some challenges in finding the appropriate SDC form [54]. Beside high efficiency of the SDRE method in practical applications, its stability investigation encounters difficulties in the absence of proper theories in this field. The asymptotic stability constraints occasionally cause difficulties in distinguishing the SDC form [55]. However, if the system has unstable and uncontrollable modes, it can be totally stabilized by adding a stabilizer term to unstable subsystems [56] or ignoring uncontrollable modes in stable systems [57].

Stability or simplified stability of GGV dynamics can be examined with a small deviation from the equilibrium configuration. It is clear that the effects of the forces on control surfaces are negligible compared to torques. This simplified assumption is prevalent in the designing of aerial vehicle control and does not affect controllability [58]. On the other hand, aileron and rudder commands have the uppermost impression in roll and yaw moments respectively; but their

little influence on pitch is deniable. Hence, the elevator is the main factor in pitch moment changes. With this analysis, the relative independence of control commands from to each other and, consequently, from the implicit controllability of the matrix pair $(A(x) . B(x))$ can be concluded. According the principles of system identification, if the dynamic that should be identified is stable and identification error remains bounded, the identified system will be stable. Earlier, some points were presented about stability of online ANFIS identifier. On the other hand, for a wide range of data, convergence identified output to real output can be interpreted that identified relations for the A and B matrices and the F vector have minimum admissible error. Therefore, the controllability of the real dynamic is equivalent to the identified dynamic's controllability.

Despite all the mentioned difficulties, the SDRE control method has fascinated researchers and engineers compared to other nonlinear control approaches like feedback linearization [59].

B. CLOSED-LOOP STABILITY ANALYSIS

As mentioned above, stability assurance to convince all control subjects is the most important challenge. The stability of the outer loop is investigated in Theorem 1 before studying hybrid framework stability in the Theorem 2.

Theorem 1: Dynamic system (36) controlled by (39) satisfies all control objectives, and the error of angular positions tend global asymptotically to zero.

Proof: Stability of the outer loop can be easily established using mechanical energy as the Lyapunov function candidate. The positive definite function is supposed in the following form:

$$V(x_{out}) = \frac{1}{2} x_{out}^T P_{out} x_{out} \tag{42}$$

Differentiating the storage function (42)

$$\dot{V}(x_{out}) = \frac{1}{2} \dot{x}_{out}^T P_{out} x_{out} + \frac{1}{2} x_{out}^T P_{out} \dot{x}_{out} \tag{43}$$

Replacing the control law (39) in (36) and substituting (36) in (43) is concluded as

$$\dot{V}(x_{out}) = -x_{out}^T P_{out} B_{out}(x_{out}) R_{out}^{-1}(x_{out}) B_{out}^T(x_{out}) \times P_{out} x_{out} \tag{44}$$

Given the property of positive definite functions, $H(x_{out}) = P_{out} B_{out}(x_{out}) R_{out}^{-1}(x_{out}) B_{out}^T(x_{out}) P_{out}$ is a positive definite term. Thus:

$$\dot{V}(X_{out}) = -X_{out}^T H(X_{out}) X_{out} < 0 \tag{45}$$

In the case of a negative definition of the Lyapunov function candidate differentiation, boundedness of energy function and asymptotic stability of system are presumable. Additionally, it can be deduced that the Lyapunov function (42) is radially unbounded and globally stable.

Definition: A dynamic system is considered as the following model:

$$\begin{aligned} \dot{x} &= f(x.u) \\ y &= h(x.u) \end{aligned} \tag{46}$$

where $f : R^n \times R^m \to R^n$ is locally Lipchitz, $h : R^n \times R^p \to R^p$ is continuous and $h(0.0) = 0, f(0.0) = 0$. System (46) is strictly passive if there is a positive semi-definite differentiable continuous function V(x) such that for the positive definite function $\psi(x)$, the next relationship is satisfied:

$$u^T y \geq \dot{V} + \psi(x) \tag{47}$$

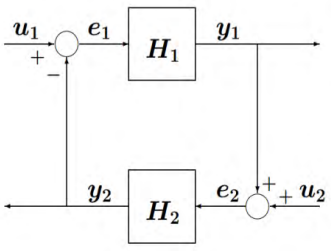

FIGURE 8. Feedback connection.

Lemma 1: For the closed-loop system similar to the one in Fig. 8, dynamic systems H_1 and H_2 have the conditions of definition (46)*, If H_1 and H_2 are passive (strictly passive), their feedback connection is also passive (strictly passive). Detailed proof of this lemma is given by Khalil [60].*

Theorem 2: Dynamic system (36) controlled by (39) is strictly passive.

Proof: Dynamic (39) can be rewritten to the form (48)

$$\begin{aligned} \dot{x}_{out}(t) &= B_{out}(x_{out}) u_{out}(t) \\ &= -B_{out}(x_{out}) R_{out}^{-1}(x_{out}) B_{out}^T(x_{out}) P_{out} x_{out}(t) \\ Y &= U = -R_{out}^{-1}(x_{out}) B_{out}^T(x_{out}) P_{out} x_{out}(t) \end{aligned} \tag{48}$$

The establishment of all the above defined conditions for this dynamic system depends on finding the storage function, $V(x)$. The boundedness of matrix B_{out} can be simply proved since system function (f) is Lipchitz. Simplifying the left side of inequality (47)

$$U^T Y = U^T U = X_{out}^T H(X_{out}) H^T(X_{out}) X_{out} \geq 0 \tag{49}$$

Defining $\psi(x) = X_{out}^T \Omega X_{out}$ such that positive definite matrix Ω satisfies the condition (50), Lyapunov function (42) is the storage function corresponding to the definition. Consequently, the outer closed-loop system is strictly passive.

$$H(X_{out}) - \Omega \geq 0 \tag{50}$$

Theorem 3: On the assumption of inner-loop passivity, closed-loop system (10) *controlled by* (32) *(Fig. 6) is stable.*

Proof of Theorem 3: It is clear that the system control block diagram (Fig. 6) is similar to the feedback connection described in Fig. 8 by considering H_1 as the outer loop

dynamic and H_2 as inner-loop dynamic. In this case, the conditions of Theorem 1 can be held under the passivity of both subsystems, while the overall system is stable.

VIII. NUMERICAL SIMULATIONS

The suggested hybrid framework was simulated to evaluate controller performance for a GGV. The main objective of the simulation is to describe the speed of the identifier in determination of the SDC form and its effect on controlling resistance performance in the presence of disturbances and noise measurement on target tracking.

Required to use the proposed control method, the availability of all system states is required. Extremely IMU accurate and fast sensors are used to measure angle and angular velocity and, GPS is used to measure linear position and velocity. Typically, IMU sensors have a precision of 0.01-0.1°, where sampling frequency provide data until 400 Hz through an RS422 serial interface [61]. However the work frequencies in GPSs are usually less than 10 Hz, and their measurement accuracy varies with product quality.

In this paper, sensors measurement error is considered as noise in simulations, so that the performance of the simulated system will be closer to reality. The measurement error for the IMU sensor is 0.1° and for the GPS is 1 m, which has been modeled as white noise with zero mean. The sampling time for the IMU sensor is 0.005 s and for GPS 0.2 s which is equivalent to 200 and 5 Hz, respectively.

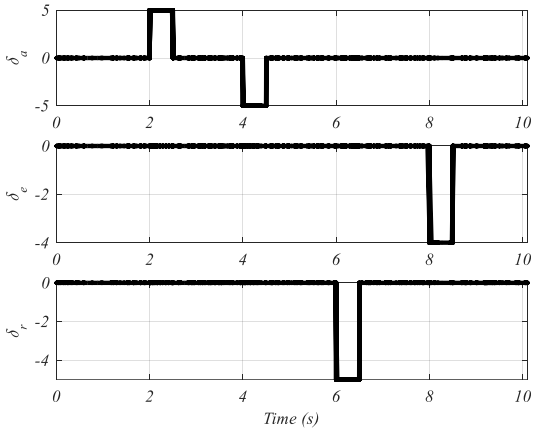

FIGURE 9. Input for validation online-ANFIS identifier performance.

The simulated GGV has a weight of $m = 90\,Kg$, wing span of $b = 1.45\,m$, and average cord length of $\bar{c} = 0.17\,m$. At first, the PSO algorithm tunes offline ANFIS network based on a set of stored data from control inputs and states. Training data are collected from the optimal solution in tracking a stationary target in the absence of any turbulence. In fact, efforts were made to as much rich data as possible that includes all UAV behavior during tracking. As seen in Fig. 9, the step input was applied to the system that verifies identifier reaction in online adjustment and evaluates initial training. Definition step input not only demonstrates identification accuracy but also responds to speed in the case

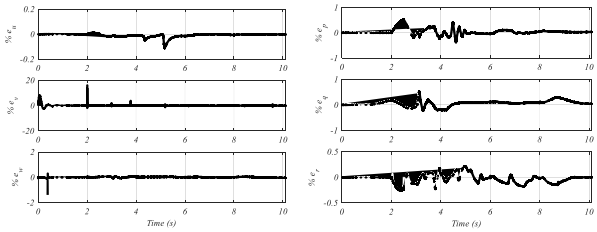

FIGURE 10. The states' identification percent error.

of sudden turbulence and commands. Relative identification percentage error (Fig. 10) proves the claim of online ANFIS identification ability.

Since the identifier goal in this problem is appropriate determination of the matrices A and B, controller performance in GGV trajectory tracking is representative of this ability. After training, the initial network is put inside the control loop.

To set weighting matrices and online learning constants, the control framework efficiency was evaluated in two different cases. It should be noted that all tests were done in the presence of atmospheric turbulence. In the first case study, the position of the target was assumed to be constant. In the second scenario, the GGV had to track a moving target like a landing platform on a ship deck or a mobile vehicle. These simulations indicated the general performance of the recommended scheme in terms of stability, robustness, and error boundedness.

In order to illustrate the importance and impact of SDC matrices on controller performance and closed loop system behavior, the proposed SDC matrix online identification method is compared with the model presented in [62].

The important point in determining the initial conditions is the initial GGV velocity that is equivalent to reference vehicle velocity at the moment of release. This velocity must be more than the GGV's stall speed and proper release speed, depending on the maneuver speed of the target and GGV ability.

A. ATMOSPHERIC TURBULENCE

Atmospheric turbulence, consisting of air mass movements, affects the efficiency and easy handling of aerial vehicles. Two main models are generally used to simulate gusts: 1-cos model and sharp-edge gust. The occurrence of both models is probable; however, harmonic gusts have priority compared to real industrial methods in implementation [63]. Owing to the specific gust speed profile in ideal sharp edge, this kind of wind rarely happens in nature [64]. The simulations are exerted in the presence of harmonic gusts that show the effectiveness of the hybrid control framework.

Evaluation of the robustness of the suggested control scheme in facing turbulence is required for modeling the real behavior of atmospheric conditions. In practical terms, with regard to the absence of the possibility of deterministic prediction of air molecule behavior, statistical descriptions are

used to categorize the intensity and spectral characteristics of turbulence. From Von Karman and Dryden wind turbulence models, the Dryden spectrum has priority because of simpler simulation possibilities [65].

According to Dryden's studies [66], and considering limited white noise, angular and linear velocities of stochastic model of wind is determined proportional to the flight altitude, velocity profile, and the GGV orientation added to simulations.

Turbulence air not only includes waves with a frequency but a full spectrum of frequencies. According to the mentioned standard, spectral function in longitudinal direction is

$$\phi_{u_g}(\omega) = \frac{2\sigma_u^2 L_u}{\pi V} \frac{1}{1+\left(\frac{L_u\omega}{V}\right)^2}$$
$$\phi_{p_g}(\omega) = \frac{\sigma_w^2}{VL_w} \frac{0.8\left(\frac{\pi L_w}{4b}\right)^{1/3}}{1+\left(\frac{4b\omega}{\pi V}\right)^2} \quad (51)$$

where b is the wing span of vehicle, V and L are the vehicle's velocity and the length of turbulence scale and the standard deviation σ is a function of altitude and turbulence intensity. The subscripts "u," "v" and "w" are referred to as the longitudinal, lateral, and vertical directions of the aerial vehicle. The spectral density of longitudinal turbulence angular rates is a partial differential of velocities in other directions.

$$p_g = \frac{\partial w_g}{\partial y} \quad (52)$$

Transfer functions of velocities are also defined as bounded subtraction functions. Other spectral functions are also stated in [66].

B. CASE 1: ROBUST TRACKING TARGET WITH MINIMUM POSITIONING ERROR

First, the simulation concentrates on evaluating the robustness of the suggested framework in the presence of turbulence. In this simulation, the initial velocity of GGV is $160\,m/s$ and height 2200m at the release point, and the stationary ground target is placed at 3700m. For this purpose, the weight coefficients for achieving the best performance and the lowest tracking error relative to the fixed target was defined.

Then it is assumed that the gust $1-\cos$ has been applied at 10 to 15 s interval to the GGV from the front. The effect of this gust on Euler's angles and the target orientation error is shown in Fig. 11 and Fig.12 Due to the fact that the gust is only applied to the GGV from the front, its effect is only evident at an angle θ. After the release, the GGV is quickly seen on the line of sight and continues its path without any error before the gust. However, at the 10 to 15 s interval, the GGV nosepiece swings high and low due to the presence of a sinusoid gust. The result of the changes in this direction causes harmonic angular velocity around the y axis to result in linear velocity changes along x and z (Fig. 13).

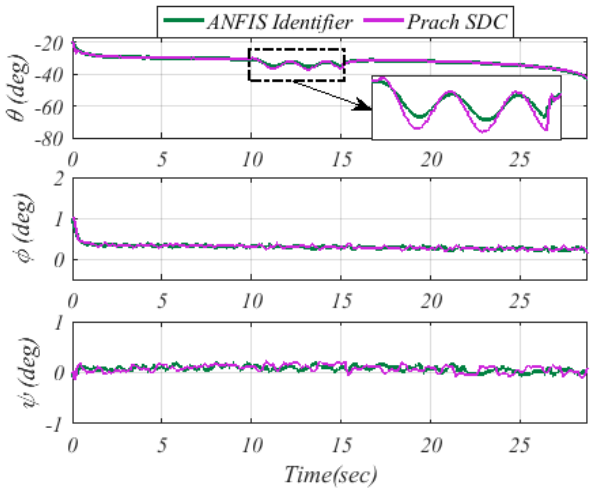

FIGURE 11. GGV's euler angles in the presence of gust.

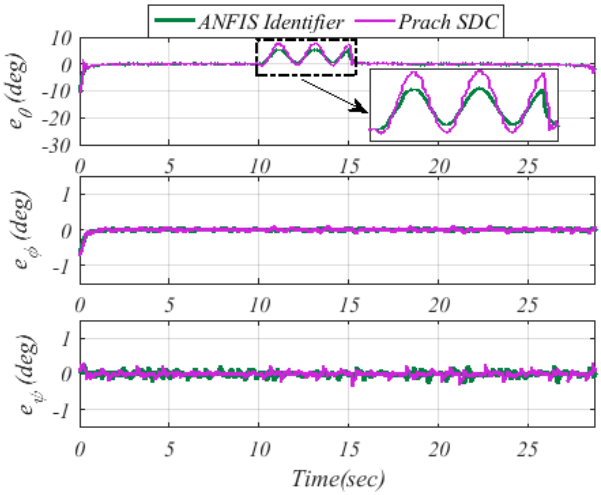

FIGURE 12. Tracking position errors in the presence of gust.

Control commands have been shown in Fig. 14. At the moment of release, control commands experience sudden changes, due to the controller's effort to correct the orientation toward the target and; after placing on the target path, the average value of control commands reaches zero. However, in the 10 to 15 s interval, changes are observed in the elevator control command, due to the impact of the gust on the GGV nose. In justifying this behavior, it is necessary to examine the 10 to 15 s interval in three periods.

As shown in Fig. 11, the gust at 10 s causes a sudden drop in the angle θ. This action makes the elevator control command in the face of this sudden change behave in such a way that the GGV nose goes upwards and the tracking error is corrected.

In the 10 to 15 s interval, due to harmonic changes at angle θ, the elevator control command also changed with the same frequency. But at 15 s, the elevator control command prevented the nose from rising suddenly by applying a

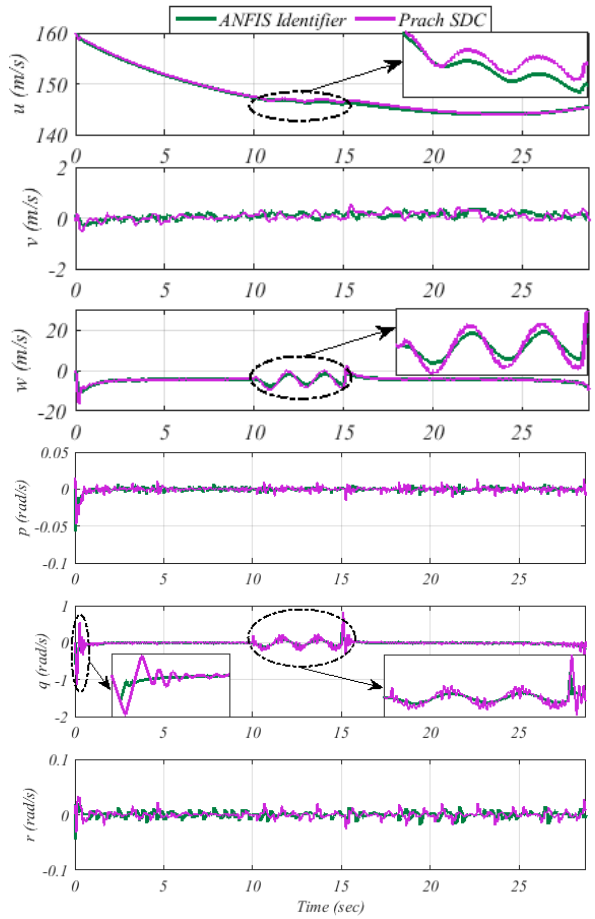

FIGURE 13. GGV's velocities in tracking fixed target in the presence of gust.

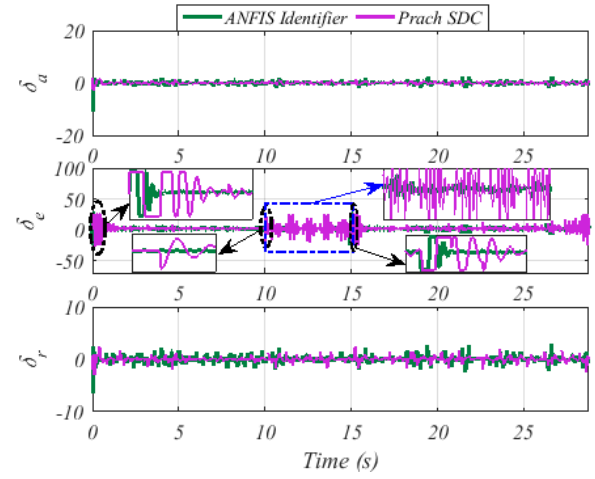

FIGURE 14. Control surface commands in tracking fixed target.

negative angle to the GGV. This change is due to the fact that the force applied to the nose by the gust suddenly disappeared.

After 15 s, the average value of the elevator control command reached zero again, and the controller was able to reset the tracking error to zero (Fig. 12).

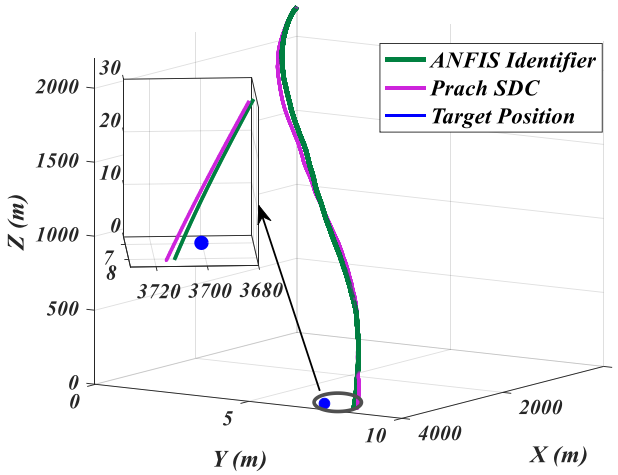

FIGURE 15. Tracking CGV positioning despite gust blowing.

Fig. 15 shows how to trace the target line of sight with the GGV. The trajectory of the path to the target and tracking with the lowest arrival error (10.2 m) indicate high strength and speed of the identifier in dynamic approximation in the presence of disturbances.

In accordance with Fig. 12 to Fig.15, despite the gust at the 10-15 s time interval during motion, track tracing is quite evident. The GGV is quickly targeted at the line of sight and remain in this direction until reaching the target (Fig. 15). From this perspective, the controller has the ability to track the entire path (Fig. 12).

Online detection of SDC matrices, in addition to reducing the disturbance effect on closed loop system states implied that the controller surfaces (with less changes and less energy than the method presented in [62] directed the GGV towards the target. In addition, the elevator control command is zero after sudden changes at the moment of application and destruction of the gust; faster than the method presented in [62] and in 10 to 15 s interval, it also behaves better with less sudden changes.

After assuring the ability of the controller to eliminate external disturbances and their effects on the final range, a turbulent flow is simulated at speed of $30m/s$. Due to the short duration of flying, it is assumed that there is a simulated wind speed along the path. Fig. 16 and Fig.17 Show the simulated wind speed and angular momentum in accordance with the Dryden statistical model along the path.

Despite applying such turbulence, appropriate GGV control inputs preserve it on the optimal path and help it reach the target in the distance of 15m (Fig. 18). The rapid elevator response could be repressed by the effects of turbulences on the aerial vehicle's movement and maintained the GGV direction. Non-smoothing control inputs related to variable amplitudes and frequencies of modeled disturbances is plotted in Fig. 19 This, in the first place, shows high potency and velocity of identifier reaction, and controller robustness in the presence of external turbulences, in the second.

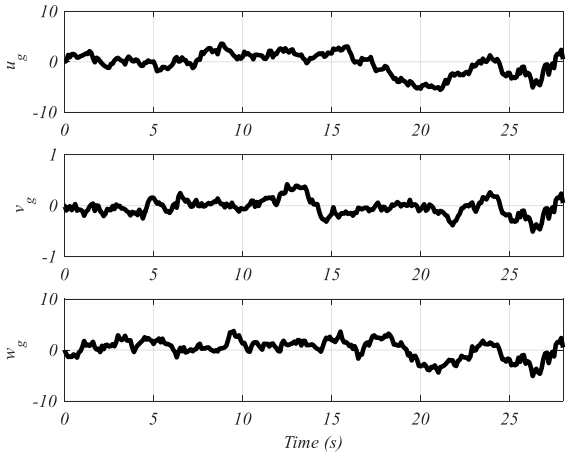

FIGURE 16. Turbulence velocities.

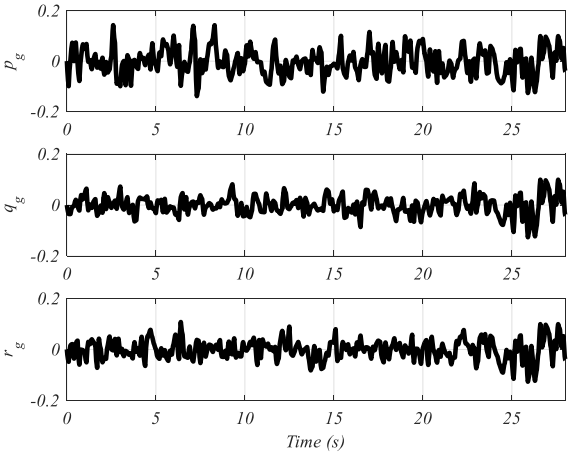

FIGURE 17. Turbulence angular rates.

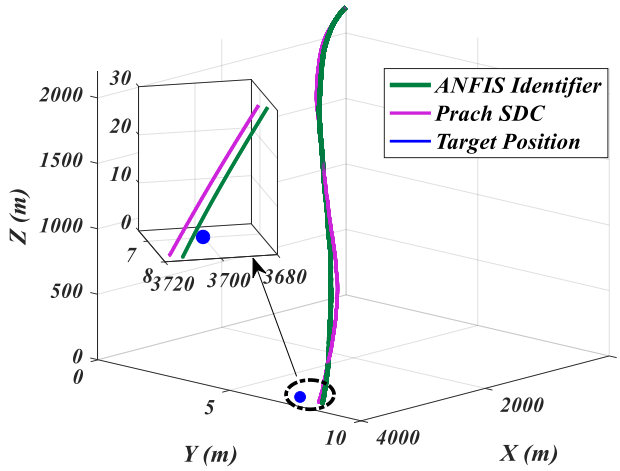

FIGURE 18. Tracking GGV positioning despite wind turbulence.

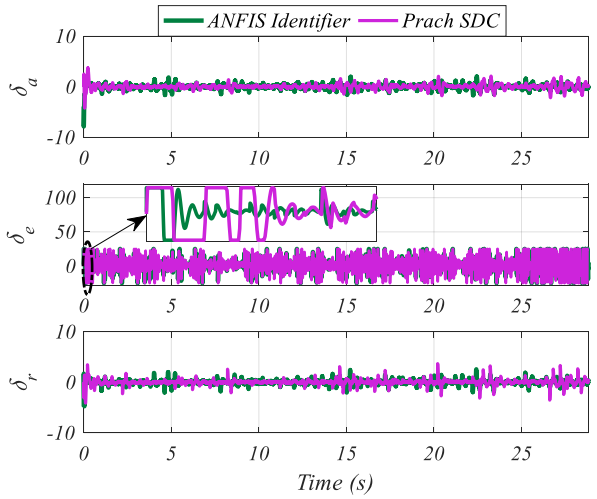

FIGURE 19. Control surface commands for atmospheric turbulence rejection.

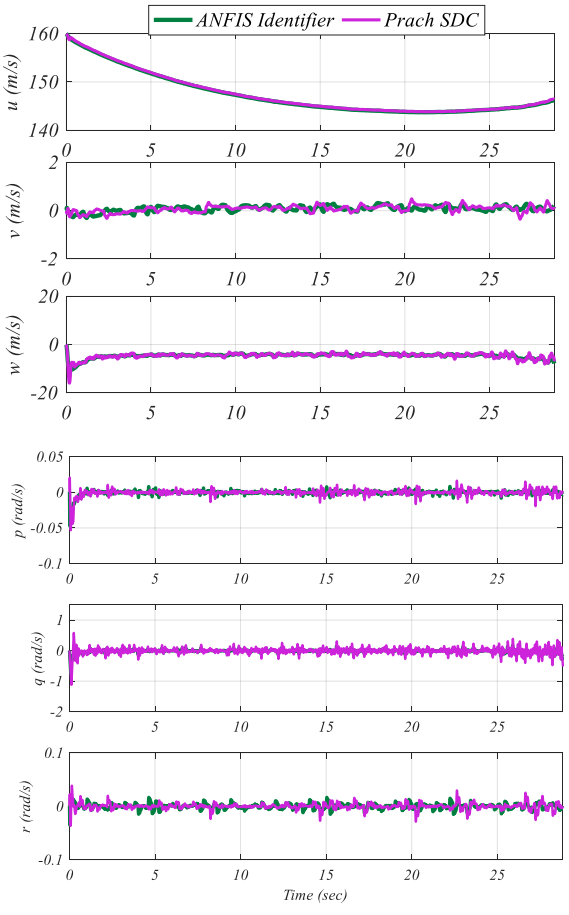

FIGURE 20. GG's states in the presence of atmospheric turbulence.

Fig. 20 illustrates the effect of control commands on states for achieving the smooth path toward target.

The matched identifier output with real output demonstrates the high speed of the identifier in tracking changes (Fig. 21). Even in the moments that high oscillation of the system, output and, consequently, identifier, is reported, error amplitude does not violate an acceptable level. However, the identifier is not trained for such situations and the initial training data have been without any noise

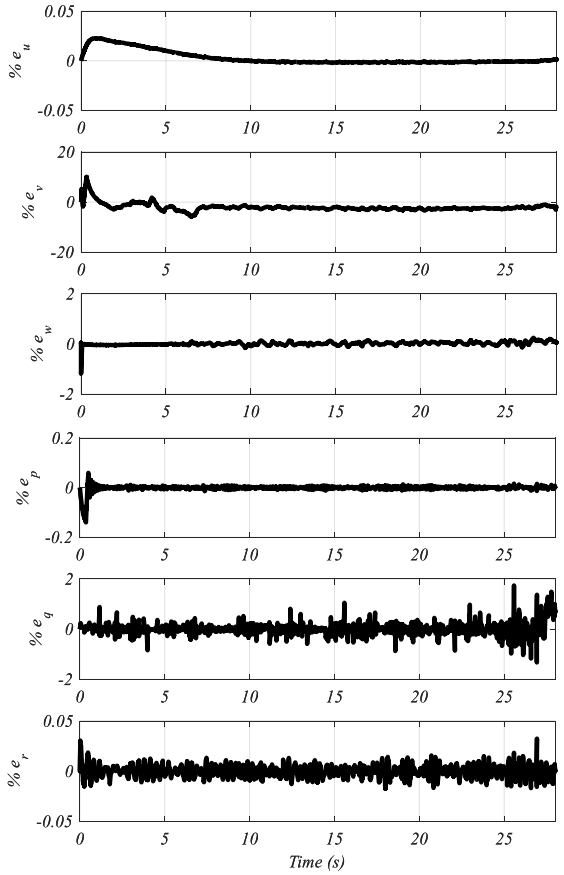

FIGURE 21. States' identification errors.

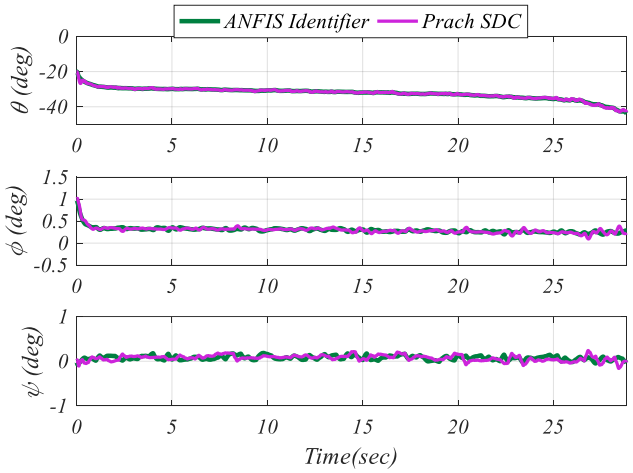

FIGURE 22. GGV's euler angles in tracking target.

and turbulence. Therefore, the identifier robustness during atmospheric turbulence is attributable in addition to control robustness.

Guidance and orientation error of GGV toward target is also evident in connection with the claim that the online ANFIS network identifier and suggested control framework have strong potentials (Fig. 22 and Fig. 23).

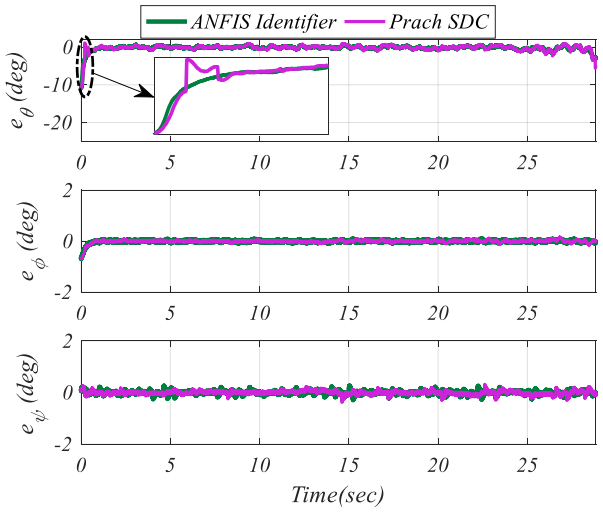

FIGURE 23. Angular tracking errors in turbulence presence.

C. CASE 2: TRACKING MOVING TARGET IN PRESENCE OF EXTERNAL DISTURBANCES

The second scenario, which is designed for tracking a moving target, shows how the proposed framework can be successfully implemented in real applications. The target is moving north east at a constants speed $14\,m/s$ and $5\,m/s$ in the direction X and Y, respectively. GGV is released at a height of 3200m and a distance of 8200m from the target with velocity $165\,m/s$. This expansion case study is also provided with air disturbances to practically investigate the effectiveness of the proposed control strategy. The velocities and the rate of angular changes of the modeled wind during the time are depicted in Fig. 24. The goal of applying this turbulence is to show the online structural ability of ANFIS in identification and controller ability in suppressing turbulence effects with high changes of amplitude during the application time.

Unlike the previous state, the path that the GGV traversed to reach the target also had variations along the y axis (Fig. 25). Fig. 26 justified this behavior. The GGV, after a short period of release moment will be at the desired angles and when the tracking error reached zero (Fig. 27). Roll and Yaw angles adjusted the GGV in y-axis and given that the target in the y axis has velocity, therefore, roll and yaw angles also increased in the direction of tracking the target. This process continues for 35 s, and the GGV continues to move steadily without any changes in angular velocity (Fig. 28).

But at 35 s, the optimal roll angle is zero and the yaw angle decreases. This is due to GGV overtaking the moving target due to high velocity of the GGV. At 35 s interval, GGV could compensate for the distance in the y and x axes. As a result, the GGV in the y axis moves forward from the target and the desired angles change in accordance with the relationships of the guidance section.

However, at 47 s, the desired angles of roll and yaw increase such that the target overtakes along the Y axis. This behavior occurs several times before the moment of collision which is mainly due to the moving target which causes the

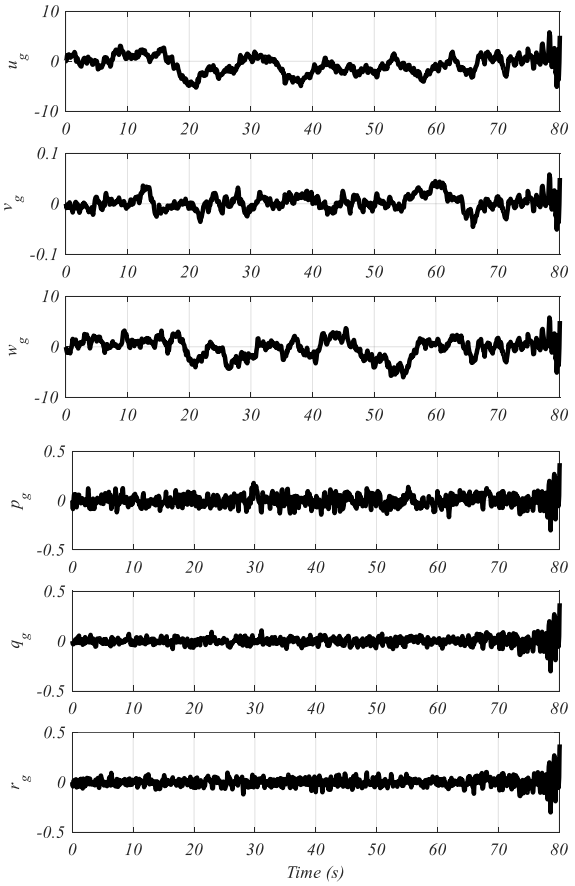

FIGURE 24. Wind turbulence velocities and angular rates.

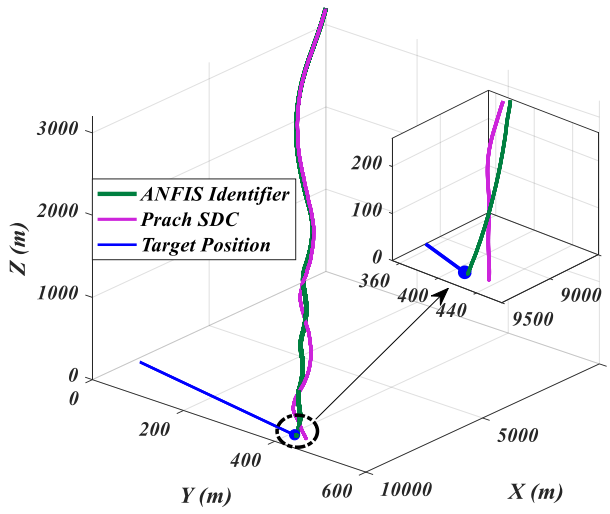

FIGURE 25. Positioning GGV in tracking moving target despite wind turbulence.

GGV's forward and backward movement toward the target in the direction of the y axis.

The changes made to the roll and yaw angles cause linear velocity changes in the y axis and angular velocities around the x and z axes (Fig. 28). By changing the angular velocities, the system is removed from the stable state.

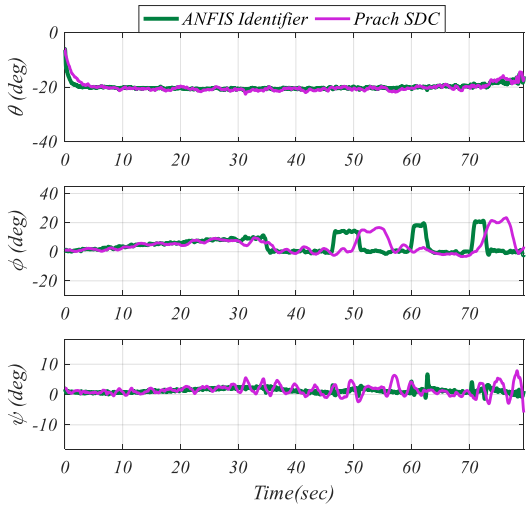

FIGURE 26. Angular tracking of moving target despite wind turbulence.

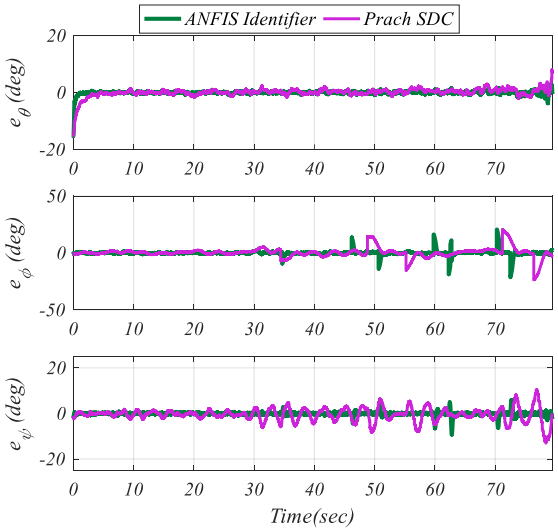

FIGURE 27. Wind turbulence effect on positioning in tracking target.

Therefore, the controller must restore the system to a stable state, in addition to reducing tracking error. Under these conditions, the duty to modify these changes is on the aileron and rudder control commands.

As shown in Fig. 29, aileron and rudder control commands suddenly changed precisely at the moments when the desired angles were changed which causes the stability of the angular velocities and thus provides the optimal tracking.

According to Fig. 25 to Fig. 29, the identifier has been able to follow the moving object even in the event of disturbances and arrives at an acceptable accuracy to the designated point.

Owing to low speed response of the system dynamic, high oscillations and fast control commands could not disturb the smooth resultant behavior of the system (Fig. 28). GGV tracks target by trying to get equivalent velocity of target movement in the Y direction and increasing velocity in the X direction than in the previous case (stationary target).

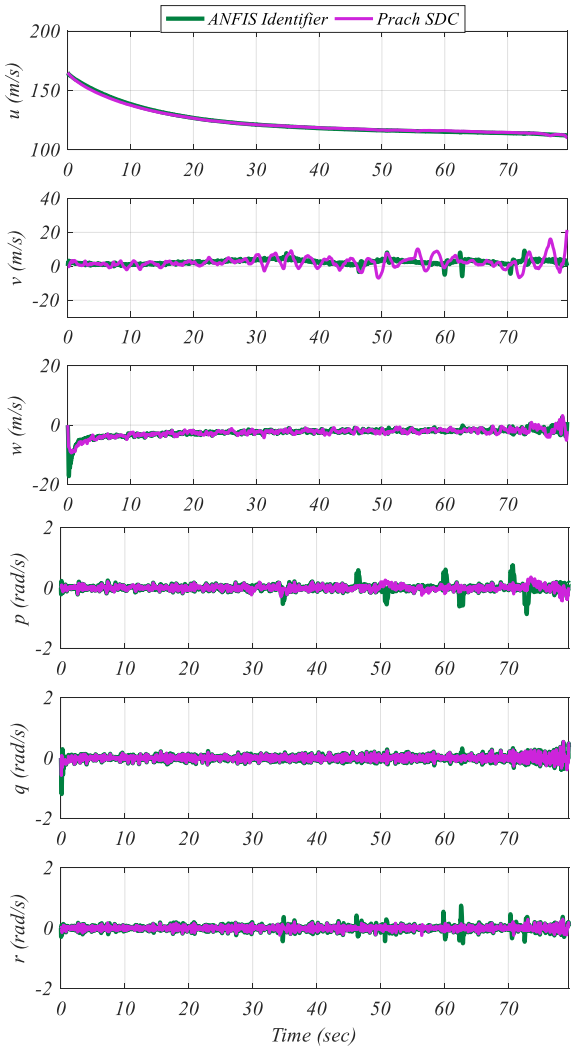

FIGURE 28. Dynamic system response due to wind turbulence.

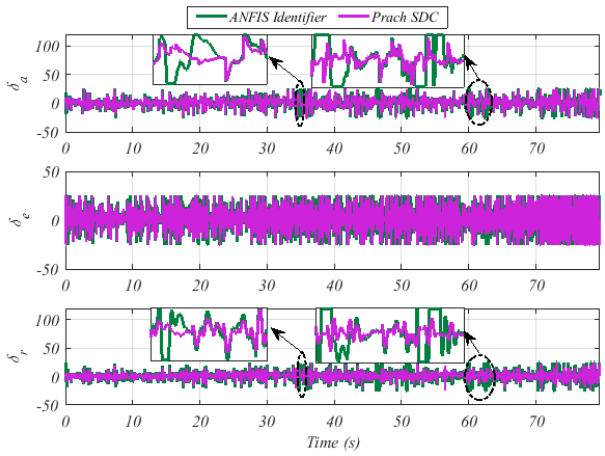

FIGURE 29. Turbulence effect on flight control commands.

Generally, the performance of the identifier in determining states is defendable (Fig. 30) and the identification error is increased only in the case of sudden changes in the value or direction of variables. With respect to the simulations

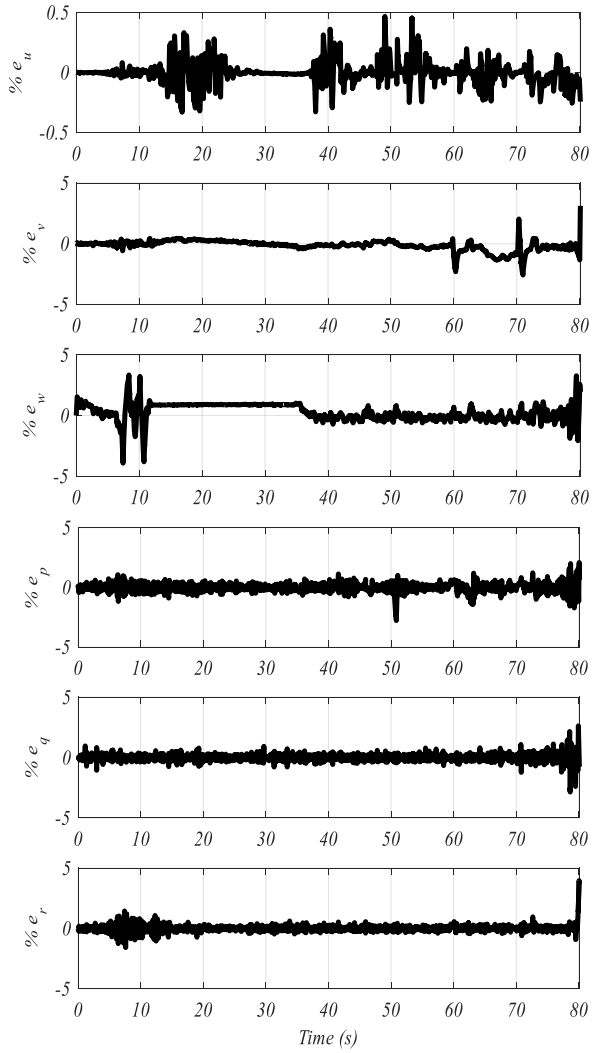

FIGURE 30. Identifier percentage errors.

of the previous stage, error amplitude is increased because of an absence of initial training identifier for such a situation. In addition, the highest percentage of relative identifier error is about 4%; while the identification error is less than 1% unless in short times. This means that the identifier could be updated to match dynamic behavior under turbulence with high amplitude and frequency, and tracking a moving target. This result highlights the practical aspect of this structure.

IX. CONCLUSION

In this paper, a novel hybrid optimal control design for GGVs is presented under uncertainties and in the presence of environmental turbulence. The presented framework includes the SDRE feedback controller for state regulation in the inner loop, which is incorporated with the optimal guidance law outside this loop. On the other hand, utilizing the high potential of the ANFIS network in identifying nonlinear complex functions, an innovative method for online continuous identification of dynamic systems is introduced for the first time. This strategy establishes an appropriate SDC form for inner controller loop by means of filtering nonlinear dynamic, mod-

ifying online error in the back propagation training algorithm and initial offline PSO for learning algorithm. Therefore, the exact model of system dynamic, uncertainties, and turbulence could be removed. Although GGVs are unpowered systems, the tracking of the optimal path involves minimizing the control effort and the positioning error related to the initial conditions.

Comprehensive stability analysis of the entire closed-loop system is performed. According to the theoretical investigation, all system states will remain bounded, if the dynamic of the system is essentially stable. Furthermore, the target positioning error converges on the minimum acceptable level on the passivity assumption of the inner loop. In addition, the robustness of this approach is guaranteed under external disturbances included atmospheric turbulence and uncertainties.

The new control scheme on a GGV is carried out in the presence of external turbulence. Subsequently, training initial ANFIS network with PSO algorithm, the identifier is placed in the inner loop. Implementing assorted atmospheric turbulence, tracking and guidance toward stationary and low maneuverable target are investigated. The results successfully demonstrate the effect of online identification of the SDC form and nested SDRE control framework in minimizing control effort, diminishing positioning error, and tracking the optimal path into target.

The simulation results show the successful effect of online identification of the SDC form and combined SDC control in minimizing the controlling effort, reducing target error, and navigating the optimal path to the target as compared to previous approaches.

The setting of weighting matrices for achieving the best performance of the SDRE control is the limitation of this technique. Hence, recommending a proper model for predicting the optimum values of these parameters would not only speed up the design process but also enhance the capability of practical implementation of this method. The feasibility of this idea should be a concern of future studies.

REFERENCES

[1] F. Jahangiri, H. A. Talebi, M. B. Menhaj, and C. Ebenbauer, "A new approach for minimum phase output definition," *Int. J. Syst. Sci.*, vol. 48, no. 2, pp. 264–271, 2017.

[2] D.-C. Zhang, Q.-L. Xia, Q.-Q. Wen, and G.-Q. Zhou, "An approximate optimal maximum range guidance scheme for subsonic unpowered gliding vehicles," *Int. J. Aerosp. Eng.*, vol. 2015, Nov. 2015, Art. no. 389751. [Online]. Available: https://www.hindawi.com/journals/ijae/2015/389751/abs/

[3] Z. Yu, C. Jing, and S. Lincheng, "Real-time trajectory planning for UCAV air-to-surface attack using inverse dynamics optimization method and receding horizon control," *Chin. J. Aeronautics*, vol. 26, no. 4, pp. 1038–1056, 2013.

[4] A. S. Attallah, G. A. EL-Sheikh, A. T. Hafez, and A. S. Mohammady, "Attitude control of gliding bomb using classical PID and modified PI-D controllers," *J. Multidiscipl. Eng. Sci. Technol.*, vol. 3, no. 4, pp. 4451–4456, 2016.

[5] A. S. Attallah, "Modeling and simulation for free fall bomb dynamics in windy environment," in *Proc. Aerosp. Sci. Aviation Technol.*, Cario, Egypt, 2015, pp. 1–13.

[6] R. Pepy and B. Hérissé, "An indirect method for optimal guidance of a glider," *IFAC Proc. Vol.*, vol. 47, no. 3, pp. 5097–5102, 2014.

[7] A. Wernli and G. Cook, "Suboptimal control for the nonlinear quadratic regulator problem," *Automatica*, vol. 11, no. 1, pp. 75–84, 1975.

[8] T. Çimen, "Systematic and effective design of nonlinear feedback controllers via the state-dependent Riccati equation (SDRE) method," *Annu. Rev. Control*, vol. 34, no. 1, pp. 32–51, 2010.

[9] Y. Sakayanagi, D. Nakayama, S. Nakaura, and M. Sampei, "Clarification of free parameters of state-dependent coefficient form: Effect on solving state-dependent Riccati inequality," *IFAC Proc. Vol.*, vol. 41, no. 2, pp. 182–187, 2008.

[10] J. Cloutier and D. Stansbery, "All-aspect acceleration-limited homing guidance," in *Proc. AIAA Guid., Navigat., Control Conf.*, Portland, OR, USA, 1999, p. 633.

[11] J. R. Cloutier and P. H. Zipfel, "Hypersonic guidance via the state-dependent Riccati equation control method," in *Proc. IEEE Conf. Control Appl.*, Kohala Coast, HI, USA, Aug. 1999, pp. 219–224.

[12] S. Kumbasar, "Nonlinear guidance and control of leader-follower UAV formations," Ph.D. dissertation, Aerosp. Eng. Dept., Middle East Tech. Univ., Ankara, Turkey, 2015.

[13] O. Tekinalp and S. Kumbasar, "SDRE based guidance and flight control of aircraft formations," in *Proc. AIAA Guid., Navigat., Control Conf.*, Kissimmee, FL, USA, 2015, pp. 1–19.

[14] H. Parwana, S. A. Varma, and M. Kothari, "An SDRE based impact and body angle constrained guidance against a stationary surface target," *IFAC-PapersOnLine*, vol.49, no. 1, pp. 1–6, 2016.

[15] J. R. Cloutier and S. Stockbridge, "Guidance and nonlinear MRAC of a powered air-to-surface weapon with terminal constraint," in *Proc. ACC*, Chicago, IL, USA, Jul. 2015, p. 2533.

[16] C. P. Mracek, "SDRE autopilot for dual controlled missiles," *IFAC Proc. Vol.*, vol. 40, no. 7, pp. 750–755, 2007.

[17] B. Geranmehr, K. Vafaee, and S. R. Nekoo, "Finite-horizon servo SDRE for super-maneuverable aircraft and magnetically-suspended CMGs," *Proc. Inst. Mech. Eng. G, J. Aerosp. Eng.*, vol. 230, no. 6, pp. 1075–1093, 2016.

[18] R. Babaie and A. F. Ehyaie, "Robust optimal motion planning approach to cooperative grasping and transporting using multiple UAVs based on SDRE," *Trans. Inst. Meas. Control*, vol. 39, no. 9, pp. 1391–1408, 2017.

[19] M. Abdelrahman and S.-Y. Park, "Spacecraft attitude control via a combined state-dependent Riccati equation and adaptive neuro-fuzzy approach," *Aerosp. Sci. Technol.*, vol. 26, no. 1, pp. 16–28, 2013.

[20] S.-W. Kim, S.-Y. Park, and C. Park, "Spacecraft attitude control using neuro-fuzzy approximation of the optimal controllers," *Adv. Space Res.*, vol. 57, no. 1, pp. 137–152, 2016.

[21] D. T. Stansbery and J. R. Cloutier, "Position and attitude control of a spacecraft using the state-dependent Riccati equation technique," in *Proc. ACC*, Chicago, IL, USA, Jun. 2000, pp. 1867–1871.

[22] N. Walia, H. Singh, and A. Sharma, "ANFIS: Adaptive neuro-fuzzy inference system-a survey," *Int. J. Comput. Appl.*, vol. 123, no. 13, pp. 32–38, 2015.

[23] A. Gite, R. M. Bodade, and B. M. Raut, "ANFIS controller and its application," *Int. J. Eng. Res. Technol.*, vol. 2, no. 2, pp. 1–5, 2013.

[24] I. D. M. Esper and P. F. F. Rosa, "Heading controller for a fixed wing UAV with reduced control surfaces based on ANFIS," in *Proc. IEEE Int. Conf. Dependable Syst. Netw. Workshops*, Jun. 2015, pp. 118–123.

[25] M. Mikhail, S. Zein-Sabatto, K. Terrell, M. Bodruzzaman, and J. Ramsey, "Reconfigurable control strategy for aircraft model operating under uncertainty," in *Proc. IEEE SoutheastCon*, Fort Lauderdale, FL, USA, Apr. 2015, pp. 1–8.

[26] A. M. Farid, "UAV controller based on adaptive neuro-fuzzy inference system and PID," *Int. J. Robot. Autom.*, vol. 2, no. 2, pp. 73–82, 2013.

[27] S. Kurnaz, O. Cetin, and O. Kaynak, "Adaptive neuro-fuzzy inference system based autonomous flight control of unmanned air vehicles," *Expert Syst. Appl.*, vol. 37, no. 2, pp. 1229–1234, 2010.

[28] M. I. Al-Saedi, H. Wu, and H. Handroos, "ANFIS and fuzzy tuning of PID controller for trajectory tracking of a flexible hydraulically driven parallel robot machine," *J. Autom. Control Eng.*, vol. 1, no. 2, pp. 70–77, 2013.

[29] K. H. Hassan, "Self learning of ANFIS inverse control using iterative learning technique," *Int. J. Comput. Appl.*, vol. 21, no. 8, pp. 24–29, 2011.

[30] M. Turki, S. Bouzaida, A. Sakly, and F. M'Sahli. "Modeling and online control of nonlinear systems using neuro-fuzzy learning tuned by meta-heuristic algorithms," *Int. J. Control Autom.*, vol.7, no. 5, pp. 323–342, 2014.

[31] B. M. Al-Hadithi, A. Jiménez, and F. Matía, "A new approach to fuzzy estimation of Takagi–Sugeno model and its applications to optimal control for nonlinear systems," *Appl. Soft Comput.*, vol. 12, no. 1, pp. 280–290, 2012.
[32] M. J. Bai and K.Sailaja, "Controller design using ANFIS-based estimation method for unmodeled dynamics," *Int. Res. J. Eng. Technol.*, vol. 2, no. 8, pp. 61–70, 2015.
[33] M. de Los Angeles Hernandez, P. Melin, G. M. Méndez, O. Castillo, and I. López-Juarez, "A hybrid learning method composed by the orthogonal least-squares and the back-propagation learning algorithms for interval A2-C1 type-1 non-singleton type-2 TSK fuzzy logic systems," *Soft Comput.*, vol. 19, no. 3, pp. 661–678, 2015.
[34] D. P. Rini, S. M. Shamsuddin, and S. S. Yuhaniz, "Particle swarm optimization for ANFIS interpretability and accuracy," *Soft Comput.*, vol. 20, no. 1, pp. 251–262, 2016.
[35] C.-F. Juang and C.-Y. Wang, "A self-generating fuzzy system with ant and particle swarm cooperative optimization," *Expert Syst. Appl.*, vol. 36, no. 3, pp. 5362–5370, 2009.
[36] G. Zhang, M. Dou, and S. Wang, "Hybrid genetic algorithm with particle swarm optimization technique," in *Proc. Int. Conf. Comput. Intell. Secur.*, Beijing, China, Dec. 2009, pp. 103–106.
[37] A. M. Farid, S. M. Barakati, N. Seifipour, and N. Tayebi, "Online ANFIS controller based on RBF identification and PSO," in *Proc. ASCC*, Istanbul, Turkey, Jun. 2013, pp. 1–6.
[38] G. M. Siouris, *Missile Guidance and Control Systems*. New York, NY, USA: Springer-Verlag, 2004.
[39] D. Ghose, "Navigation, guidance and control," Dept. Aerosp. Eng., Indian Inst. Sci. Bangalore, India, 2013.
[40] G. T. Lee and J. G. Lee, "Improved command to line-of-sight for homing guidance," *IEEE Trans. Aerosp. Electron. Syst.*, vol. 31, no. 1, pp. 506–510, Jan. 1995.
[41] J. Roskam, *Airplane Flight Dynamics and Automatic Flight Controls Pt. 1*. Ottawa, ON, Canada: Roskam Aviation Eng., 1979.
[42] H. A. Talebi, F. Abdollahi, R. V. Patel, and K. Khorasani, *Neural Network Based State Estimation of Nonlinear Systems* (Lecture Notes in Control and Information Sciences), vol. 395. New York, NY, USA: Springer, 2010.
[43] J.-S. R. Jang, "ANFIS: Adaptive-network-based fuzzy inference system," *IEEE Trans. Syst., Man, Cybern.*, vol. 23, no. 3, pp. 665–685, May/Jun. 1993.
[44] C. Xia, C. Guo, and T. Shi, "A neural-network-identifier and fuzzy-controller-based algorithm for dynamic decoupling control of permanent-magnet spherical motor," *IEEE Trans. Ind. Electron.*, vol. 57, no. 8, pp. 2868–2878, Aug. 2010.
[45] O. Hassanein, S. G. Anavatti, and T. Ray, "Black-box tool for nonlinear system identification based upon fuzzy system," *Int. J. Comput. Intell. Appl.*, vol. 2, no. 2, p. 1350009, 2013.
[46] V. G. Gudise and G. K. Venayagamoorthy, "Comparison of particle swarm optimization and backpropagation as training algorithms for neural networks," in *Proc. IEEE Swarm Intell. Symp.*, Apr. 2003, pp. 110–117.
[47] M. V. Oliveira and R. Schirru, "Applying particle swarm optimization algorithm for tuning a neuro-fuzzy inference system for sensor monitoring," *Proc. Nucl. Energy*, vol. 51, pp. 177–183, 2009.
[48] A. Chatterjee, K. Pulasinghe, K. Watanabe, and K. Izumi, "A particle-swarm-optimized fuzzy-neural network for voice-controlled robot systems," *IEEE Trans. Ind. Electron.*, vol. 52, no. 6, pp. 1478–1489, Dec. 2005.
[49] R. Kothandaraman and L. Ponnusamy, "PSO tuned adaptive neuro-fuzzy controller for vehicle suspension systems," *J Adv. Inf. Technol.*, vol. 3, no. 1, pp. 57–63, 2012.
[50] J. Kennedy and R. Eberhart, "Particle swarm optimization," *Proc. IEEE Int. Conf. Neural Netw.*, Nov./Dec. 1995, pp. 1942–1948.
[51] M. A. Shoorehdeli, M. Teshnehlab, and A. K. Sedigh, "Identification using ANFIS with intelligent hybrid stable learning algorithm approaches," *Int. J. Neural Comput. Appl.*, vol. 18, no. 2, pp. 157–174, 2009.
[52] G. De-xin and W. Rui, "A non-delay optimal disturbance rejection control approach for nonlinear systems with external disturbances and control delay," *Proc. Eng.*, vol. 15, pp. 454–458, Jan. 2011.
[53] J. R. Cloutier, C. N. D'Souza, and C. P. Mracek. "Nonlinear regulation and nonlinear H∞ control via the state-dependent Riccati equation technique: Part 1, theory," *Proc. Int. Conf. Nonlinear Problems Aviation Aerosp.*, Daytona Beach, FL, USA, 1996, pp. 1–9.
[54] H. Beikzadeh and H. D. Taghirad, "Exponential nonlinear observer based on the differential state-dependent Riccati equation," *Int. J. Autom. Comput.*, vol. 9, no. 4, pp. 358–368, 2012.
[55] S. Elloumi and N. B. Braiek, "On feedback control techniques of nonlinear analytic systems," *J. Appl. Res. Technol.*, vol.12, no. 3, pp. 500–513, 2014.
[56] D. Stansbery and J. Cloutier, "Nonlinear, hybrid bank-to-turn/skid-to-turn missile autopilot design," in *Proc. AIAA Guid., Navigat., Control Conf.*, Montreal, Canada, 2001, p. 4158.
[57] B. Friedland, *Control System Design: An Introduction to State-Space Methods*. New York, NY, USA: McGraw-Hill, 2012.
[58] M. Hammar, "Controller design for an unmanned reconnaissance aerial vehicle," M.S. thesis, School Elect. Eng., KTH Roy. Inst. Technol., Stockholm, Sweden, 2006.
[59] J. Doyle *et al.*, "Nonlinear control: Comparisons and case studies," in *Proc. Nonlinear Control Workshop Conducted Amer. Control Conf.*, Albuquerque, NM, USA, 1997.
[60] H. K. Khalil, *Nonlinear Systems*, vol. 2. Upper Saddle River, NJ, USA: Prentice-Hall, 1996, pp. 1–5.
[61] J.-H. Kim, S. Sukkarieh, and S. Wishart, "Real-time navigation, guidance, and control of a uav using low-cost sensors," in *Field and Service Robotics*. Berlin, Germany: Springer, 2003, pp. 299–309.
[62] O. Tekinalp and A. Prach, "Development of a state dependent Riccati equation based tracking flight controller for an unmanned aircraft," in *Proc. AIAA Guid., Navigat., Control Conf.*, 2013, p. 5167.
[63] A. Rigaldo, "Aerodynamics gust response prediction," M.S. thesis, School Eng. Sci., Royal Inst. Technol., Stockholm, Sweden, 2011.
[64] E. N. Abdulwahab and C. Hongquan, "Aircraft response to atmospheric turbulence at various types of the input excitation," *Space Res. J.*, vol. 1, no. 1, pp. 17–28, 2008.
[65] P. Zipfel, *Modeling and Simulation of Aerospace Vehicle Dynamics*, 3rd ed. Reston, VA, USA: AIAA, 2014.
[66] H. L. Dryden, "A review of the statistical theory of turbulence," *Quart. Appl. Math.*, vol. 1, no. 1, pp. 7–42, 1943.

MOHSEN SAYADI is currently pursuing the Ph.D. degree in aerospace structural engineering with the Tehran Faculty of New Sciences and Technologies. His Ph.D. thesis was on improving optimization methods and robust optimal control. His research interests include multidisciplinary optimization of aerospace systems, aerodynamic optimization and aerospace structures, and improve optimal and fuzzy control methods.

AMIRREZA KOSARI received the B.S. degree from Amirkabir University, Tehran, Iran, in 1998, and the M.S. and Ph.D. degrees from the Sharif University of Technology, Tehran, Iran, in 2001 and 2008, respectively. He is currently an Assistant Professor with the University of Tehran, Iran. He is an author of several papers in the areas indicated above. His research interests include trajectory optimization, optimal control, cooperative flights, and spacecraft attitude control.

PARVIZ MOHAMMAD ZADEH received the Ph.D. degree in multi-level multidisciplinary design optimization. He was an Assistant Professor with the Faculty of Aerospace Engineering, University of KNTU. He held several research positions at the School of Engineering, Design and Technology University of Bradford and the College of Aeronautics, University of Cranfield in the past. He is currently an Assistant Professor and the Director of the Multidisciplinary Design Optimization Laboratory, Faculty of New Sciences and Technologies, University of Tehran. His research interest include various aspects of multidisciplinary design and optimization of aerospace systems, complex systems design, integration, concurrent design, computational modeling, robust and reliability-based design optimization, meta-modeling, design of experiments, computational structural and stochastic analysis that leading to variety of aerospace applications.